Inter-comparison of two land-surface models applied on different scales and their feedbacks while coupled with a regional climate model

F. Zabel[1], W. Mauser[1], T. Marke[1,2], A. Pfeiffer[3], G. Zängl[3,4], C. Wastl[3,5]

[1]Department of Geography, Ludwig-Maximilians-Universität, Munich, Germany

[2]Institute of Geography and Regional Sciences, University of Graz, Austria

[3]Institute of Meteorology, University of Munich (LMU), Germany

[4]Deutscher Wetterdienst, Offenbach, Germany

[5]Department of Ecoclimatology, Technical University of Munich (TUM), Germany

Abstract

In order to study regional impacts of climate and climate change on the land surface, downstream models, are usually driven offline with results from regional climate models (RCMs). Thereby, the land surface of the downstream models is usually totally different to the land surface which is used within the RCMs. Therefore, this study compares two physically based land surface models, which developed from different disciplinary backgrounds. While the NOAH-LSM, applied in this study originally was developed for the use within the RCM MM5, PROMET was developed to answer hydrological questions on the local to regional scale. Thus, the models use different physical formulations of the land surface processes and are applied at different spatial scales of 45 km (NOAH) and 1 km (PROMET) respectively, to represent the land surface processes. The parameterization of soil and plant properties in terms of phenological behaviour and water-stress is treated with a higher level of detail in PROMET. As a result, over a four-year period for Central Europe, simulated evapotranspiration and soil moisture differs between the models both, spatially and temporally. Regions with a high proportion of impervious surfaces in PROMET show the highest differences for simulated evapotranspiration compared to the NOAH results (up to 30 %), since the NOAH land surface lacks in the option of impervious surfaces. Further, the PROMET simulation shows lower evapotranspiration rates e.g. in the Po Valley, caused mainly by a higher level of vegetation water stress in summer.

The hydrosphere at the land surface strongly interacts with the atmosphere. However, the offline coupling approach does not allow for taking feedback effects between the downstream model and the RCM into account. Therefore, we further developed an approach that allows a full interactive coupling between PROMET and the atmospheric part of MM5 by now returning the PROMET land surface energy fluxes to MM5 and thus, providing the lower boundary conditions for the MM5 atmosphere. Consequently, feedbacks and regional self-amplification effects result in increasing near surface air temperature and decreasing precipitation - especially in Southern Europe, as well as decreasing soil moisture and increasing vegetation water stress. Hence, evapotranspiration decrease with different regional and temporal behaviour.

Keywords:

Feedback Effects, Hydrological Model, Regional Climate Model, Land Surface Model, Interactive Coupling

1 Introduction

A multitude of studies deal with possible regional impacts of global climate change on land surface processes, summarized by the IPCC (2007a, b). These studies use the results of regional climate models (RCMs), which describe the processes in the atmosphere and at the land surface, thus including atmosphere interactions both for oceans and land. Modelling climate therefore always requires a representation of land surface processes within the climate model. The changing meteorological drivers are further used as inputs to downstream models, which determine the impacts of the simulated climate change on the processes of interest. Downstream models are used to analyse the impacts of climate change on a broad palette of natural and/or societal developments including the land surface water cycle, land use, agricultural yield, energy consumption and many more (Dirnböck et al., 2003; Fried et al., 2004; Haeberli and Beniston, 1998; Henderson-Sellers et al., 2008; Kalkstein and Smoyer, 1993; Mauser and Bach, 2009; Parry et al., 1999; Patz et al., 2005; Wagener et al., 2005). Thereby, they usually focus on specific thematic questions that RCMs can not or only insufficiently address, and/or focus on specific regions at high spatial resolution.

Global climate models (GCMs) have historically concentrated on modelling the largely homogeneous ocean-atmosphere interface at a relatively coarse spatial resolution, paying comparatively little attention to the land surface processes. Simplified land surface models (LSMs) have been applied in climate models that were not able to reproduce observations (Timbal and Henderson-Sellers, 1998). Regional climate models being forced with exogenous model data on the lateral boundaries of the model domain, extend the coarse description of atmospheric processes within GCMs towards increased spatial resolution and more process detail, thereby capturing the local structures at each model grid point (Giorgi, 2001; Jacob et al., 2007; Kueppers et al., 2008; Laprise, 2008; Mc Gregor, 1997; Michalakes, 1997; Quintanar et al., 2009; Schär et al., 2004; Stocker, 2004; Zampieri et al., 2011). Nonetheless, the complexity and heterogeneity of land surface processes and the need for a more detailed view on the land surface is a long standing discussion in atmospheric sciences (Dickinson et al., 1991; Dickinson, 1995; Henderson-Sellers et al., 1995; Henderson-Sellers et al., 2008). Therefore, the 'Project for Intercomparison of Land-surface Parameterization Schemes' (PILPS) fundamentally evaluated and improved physically based LSMs for the use in climate models (Dickinson, 1995; Famiglietti and Wood, 1991; Henderson-Sellers et al., 1996; Polcher et al., 1998; Timbal and Henderson-Sellers, 1998; Wood et al., 1998; Yang et al., 1998). There is evidence that more advanced and robust LSMs, which increasingly consider the spatial heterogeneity (land-use, soil, elevation) and complexity of land surface biophysical and hydrological processes in the soil-plant-atmosphere continuum on an appropriate scale will reduce the uncertainties in the current modelling of land-atmosphere processes (Essery et al., 2003; Hagemann et al., 2001; Koster et al., 2004; Laprise, 2008; Molod and Salmun, 2002; Seth et al., 1994; Yu, 2000).

Meanwhile, hydrologists have developed empirical, conceptual and more and more physically-based land surface hydrological models (LSHMs) spanning a wide range of complexity. They now go beyond reproducing runoff at gauges of small scale catchment areas by considering the catchment's hydrologic land surface processes in detail (Bharati et al., 2008; Devonec and Barros, 2002; Garcia-Quijano and Barros, 2005; Kuchment et al., 2006; Kunstmann et al., 2008; Ludwig and Mauser, 2000; Mauser and Bach, 2009; Schulla and Jasper, 1999; Wagner et al., 2009). The physically based models aim at understanding the interactions between the different land surface compartments, namely soil, vegetation, snow and ice in producing the resulting river runoff. They include detailed descriptions of vertical and lateral soil water and energy flows, vegetation dynamics and related flow regulations, snow and ice dynamics as well as energy and mass exchange with the atmosphere, and thereby cover the major land surface processes in the soil-plant-atmosphere continuum. In contrast to LSMs designed for atmosphere applications, the atmosphere is usually considered as exogenous driver only.

At the same time as RCMs have become capable of physically downscaling the GCMs outputs to a resolution of 50 - 10 km, LSHMs evolved from their original application in small watersheds to large basins. With the improving spatial resolution of the RCMs and the increasing areal coverage of the LSHMs the scales covered by the two model families tend to converge (Chen et al., 1996; Henderson-Sellers et al., 1995; Yang et al., 1998). The RCMs' outputs at high spatial resolution now allows downstream impact models on the local to regional scale to use the results of RCM simulations as offline model input (Figure 1).

Due to the different scales between impact models and RCMs and because of the huge numerical load the impacts are usually assessed with, downstream impact models are usually run offline. This means that they consider the meteorological outputs of the RCMs as exogenous input only and do not feed back to the atmosphere. However, land-atmosphere interactions are largely driven by soil moisture and soil temperature, vegetation dynamics and evapotranspiration as well as snow and ice dynamics. A lack of understanding of their complex interrelation is responsible for one of the key sources of uncertainty in climate simulations (Koster et al., 2004; Koster and Suarez, 1994; Martin, 1998; Orlowsky and Seneviratne, 2010; Pitman, 2003; Zeng et al., 2003). A consistent analysis of the regional impacts of climate change therefore would request to have the impact models directly coupled within the RCMs to be able to explicitly consider the feedback of the climate impacts on the land surface and vice versa.

The model chain when coupling a RCM with a downstream impact model offline, results in two LSMs - one within the regional climate and one within the impact model, both describing the same land surface processes. However, they are not identical which leads to inconsistencies within the offline model chain. They may have their causes in different scales between the LSMs, different coverage of land surface categories and processes, different process descriptions and different parameterizations, etc. Although these inconsistencies are hardly ever quantified, they are only justified when land-atmosphere interactions are weak.

The following analysis uses a case study to compare two LSMs, one representing a LSM used within a RCM and a hydrological downstream climate impact model. It further aims at quantifying the inconsistencies which arise from using the hydrological impact model offline in comparison to an interactively integration of the impact model in the RCM.

2 Methods

Besides the hydrological community, many disciplines have used the RCMs' outputs as input for their downstream models in the last years, e.g. for regional impact studies on plant growth, agriculture or on the economy (Myneni et al., 1997; Parry et al., 2004). These user-models also operating on the land surface thereby usually represent land surface in a totally different manner than the LSM used within the RCM. In order to describe the discrepancies and the inconsistencies between a classical LSM used within a RCM and a LSHM, we applied the fifth version of the Mesoscale Model (MM5) with the NOAH-LSM (Chen and Dudhia, 2001b) at a spatial resolution of 45 x 45 km and the LSHM from the hydrological model family PROMET (Mauser and Bach, 2009) at a spatial resolution of 1 x 1 km for the model domain of Europe. While the NOAH-LSM was originally developed for the use in regional atmosphere applications, PROMET represents a LSHM, originally designed to study the impact of climate on hydrology on the local to regional scale. Due to the different demands on each of the models, they are supposed to differ in multiple aspects. Therefore, we first describe in detail both LSMs in terms of their different scales, model physics and parameterizations. Further, evapotranspiration simulated both with the NOAH-LSM and coupled offline with PROMET (in the course of this paper named as PROMET-offline) is compared (Figure 1) for a 4-year period. Due to the equal meteorological forcings, the different models' behaviour in terms of evapotranspiration can be quantitatively investigated.

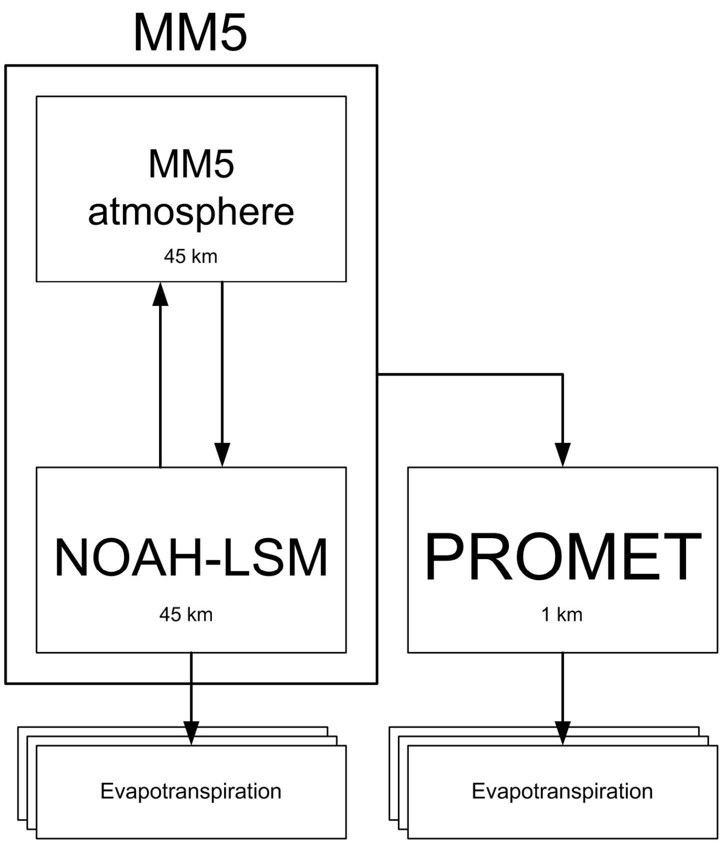

Figure 1: Principle of driving the hydrological model PROMET offline with data from the RCM MM5 within which the NOAH-LSM provides the lower boundary conditions.

Feedbacks between the downstream model and the atmosphere can not be simulated within the offline coupled approach. Downstream models which are only weakly affected by feedbacks between the land surface and the atmosphere, e.g. those who study the effect of climate change on energy demand for heating buildings, may neglect that issue. However, the hydrosphere of the land surface strongly interacts with the atmosphere (Figure 3). Therefore, this study further interactively (often also called 2-way, bidirectionally or bilaterally) couples PROMET with the atmospheric part of MM5, thereby replacing the NOAH-LSM in MM5 with PROMET. Thus, PROMET now provides the lower boundary conditions for the atmospheric part of MM5 (in the course of this paper named as PROMET-interact) (Figure 2).

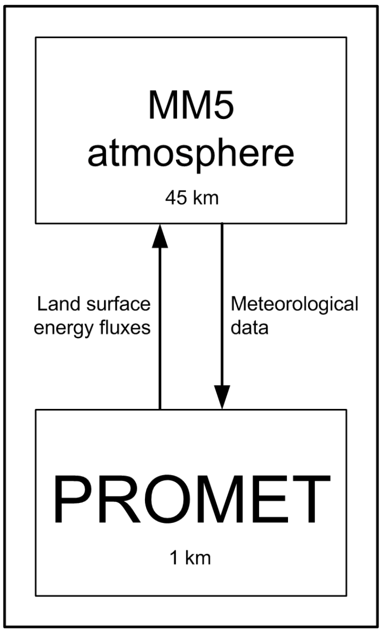

Figure 2: Interactive coupling of PROMET with the atmospheric part of MM5, thus providing the lower boundary conditions.

The substitution of the NOAH-LSM with PROMET within MM5 results in a direct interaction of the RCM with the downstream hydrological impact model and allows to analyze the inconsistencies caused by using different LSMs for the atmosphere and for quantifying the climate impacts in offline climate impact studies. Therefore, we compare the temperature and precipitation output, simulated both with NAOH-MM5 and with PROMET-MM respectively. Secondly, the PROMET evapotranspiration is compared between the offline and the interactively coupled approach.

Differences between the NOAH-LSM and PROMET concerning snow cover, wind and radiation processes due to different parameterizations and different model approaches as well as a comparison with measurements is beyond the scope of this paper but will be dealt with in further studies.

3 Study area

The study area is situated in Central Europe and extends 1170 km north-south by 1170 km east-west including 18 European countries. Plains like the Po and Upper Rhine Valley, uplands like in central Germany and mountainous regions in the Alps, which mark a climatic boundary between the temperate latitudes and the Mediterranean climate, compose a complex landscape. Altitudes are ranging from the Mont Blanc in the French Alps (4810 m) to the North Sea in the north-west and the Mediterranean Sea in the south. The area is characterized by intense agriculture especially within the fertile lowlands like the Upper Rhine or the Po Valley and densely populated areas such as the Ruhr region, Berlin, or Milan.

4 Model descriptions

4-1 The atmospheric model MM5

The RCM applied in this study is the fifth-generation Mesoscale Model (MM5) (Grell et al., 1994), developed by the Pennsylvania State University (Penn State) and the National Center for Atmospheric Research (NCAR).The widely known model has been used for numerical weather predictions, air quality studies and regional climate studies (Chen and Dudhia, 2001a).

It was modified and adapted to our specific simulation requirements and our specific model domain (Pfeiffer and Zängl, 2009; Zängl, 2002). Within the GLOWA-Danube project, in which this study took place, MM5 was applied in climate mode with a single domain having a horizontal spatial resolution of 45 km and an integration internal time step of 135 seconds in order to be able to simulate long time series for regional climate scenarios until 2100 with the available computational resources.

The MM5 domain covers most of the European continent and has a size of 79 grid-boxes in west-east and 69 grid-boxes in south-north direction (Pfeiffer and Zängl, 2009). Lateral boundary conditions are provided by 6-hourly ECMWF ERA-40 reanalysis-data (Uppala et al., 2005).

4-2 Land surface

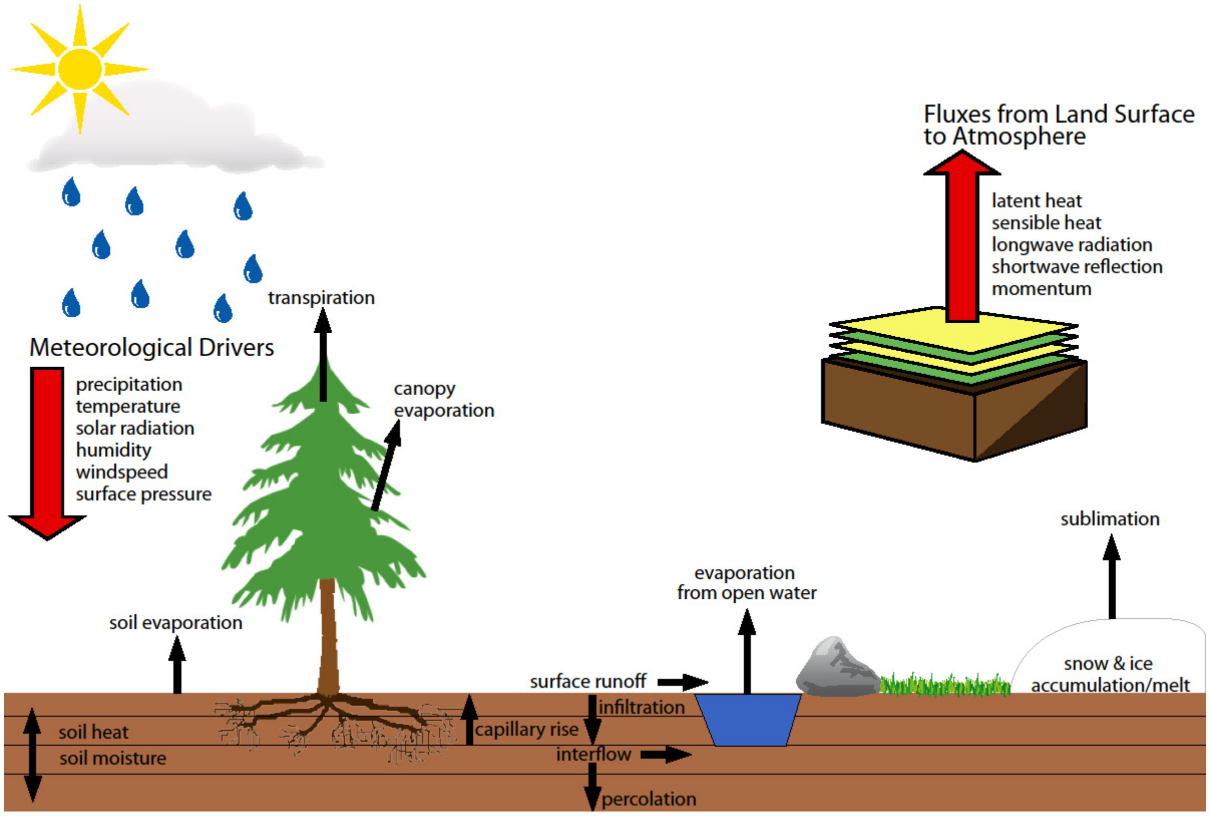

Figure 3: Scheme of water and energy fluxes on the land surface and feedbacks to the atmosphere

The LSMs applied in this study are the NOAH-LSM and PROMET. Both models describe the pathways of water and energy on the land surface in a physically based manner. The process descriptions at the land surface require meteorological drivers from the atmosphere (Figure 3) which are provided by MM5. Evapotranspiration which represents the flux of latent heat from the land surface is the main energy flux from the land surface. It is affected by all major properties of and processes on the land surface and therefore is a substantial part of both models. Thus, the main focus of the comparison between the land surface models will be on evapotranspiration.

Evapotranspiration is the sum of plant transpiration (E_t) via soil, root, leaf and the stomata and evaporation from the bare soil (E_{dir}) and evaporation of water intercepted by the canopy or other surfaces (E_i) (Eq. 1). It is driven by the gradient of vapour pressure between the surface and the surrounding air, passing the laminar boundary layer into the free atmosphere, finally carried away by the turbulent mass transport of wind within the atmospheric boundary layer expressed by the aerodynamic resistance. Thus, modelling the spatially very heterogeneous evapotranspiration is a complex issue which requires taking multiple aspects into account.

$$E = E_{dir} + E_i + E_t \tag{1}$$

The NOAH-LSM is applied at a spatial resolution of 45 km while PROMET is applied with 1 km. Therefore, the models' underlying land-use and soil information as well as the digital elevation model (DEM) vary in spatial heterogeneity. Figure 4 demonstrates this effect by comparing the land use classifications used by NOAH and by PROMET. A detailed description of the land use/cover map used in PROMET is given in Zabel et al. (2010).

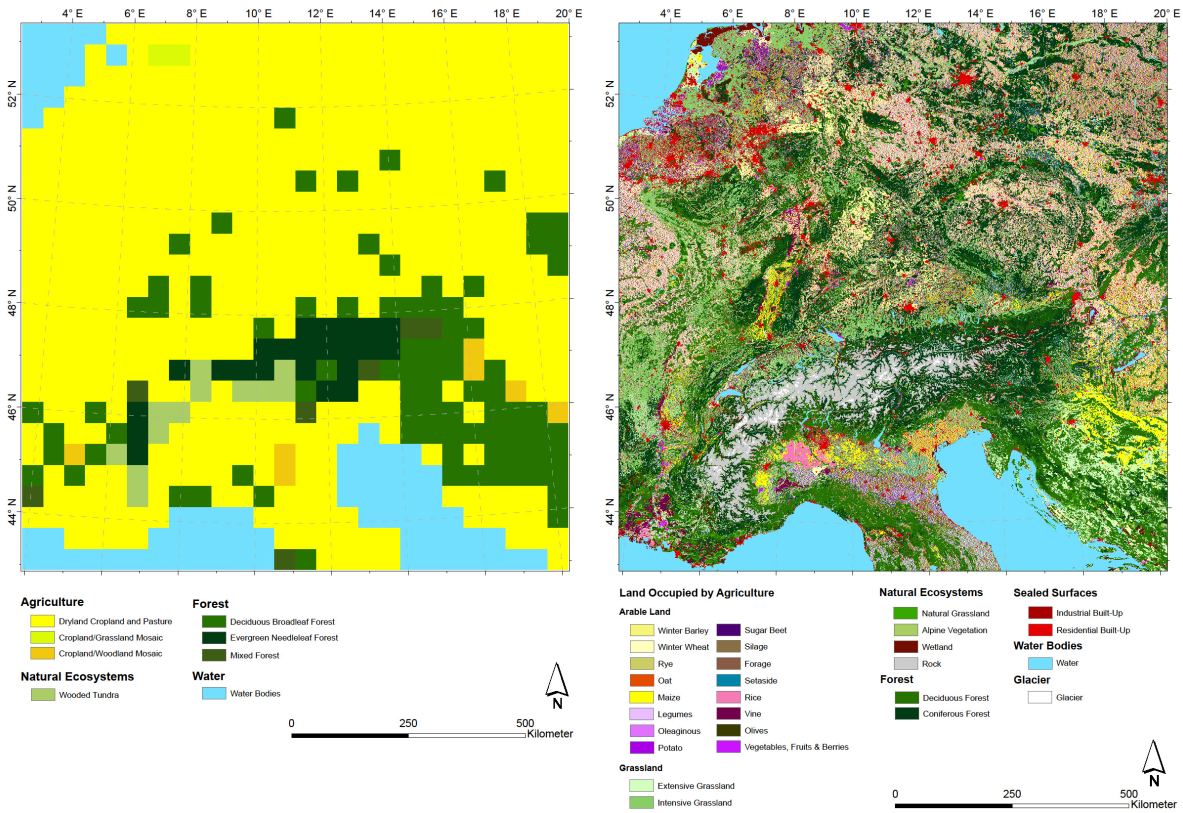

Figure 4: Land use classification of the NOAH-LSM (45x45 km) and of PROMET (1x1 km)

The land cover information has a strong effect on both albedo and partitioning of energy and matter fluxes from the surface to the atmosphere (Ge et al., 2007). Land cover determines the type of vegetation and thereby the seasonal development of plant phenology, canopy structure and leaf area, which in turn, through vegetation height and leaf area index, determines the aerodynamic and evapotranspirative properties of the land surface. The combined vegetation and soil properties determine soil moisture development and the reaction of the land surface to changing fractions of latent and sensible heat fluxes influenced by vegetation water stress.

4-2-1 NOAH-LSM

The NOAH-LSM was originally designed for the use in RCMs and is part of the MM5 modelling system. The NOAH-LSM is an updated version of the OSU-LSM. A complete description of the NOAH and OSU-LSM is given in Chen and Dudhia (2001a, b) and Mitchell (2005). The older version of MM5 documented in Grell et al. (1994), already included a simple land surface model which does not take basic hydrological effects like snow cover into account. The land use had a coarse resolution and soil moisture was defined as a function of land use with seasonal values that cannot change during the simulation or respond to precipitation. Vegetation evapotranspiration and runoff processes were not included (Chen and Dudhia, 2001a).

The goal of the development of the NOAH-LSM was to implement an appropriate LSM for weather prediction and more hydrological applications that reflects the major effects of vegetation on the long-term evolution of surface evaporation and soil moisture and to get along with relatively few parameters for short and long-time within continental-domain applications. The NOAH-LSM is the result of the further developments of LSMs, designed for atmosphere applications over the last years and scientific studies like the PILPS project.

Potential evaporation is calculated within the NOAH-LSM using a Penman-based energy balance approach (Mahrt and Ek, 1984) including a stability-dependent aerodynamic resistance. It includes a 4-Layer soil model and a canopy resistance approach of Jaquemin and Noilhan (1990) and Planton (1989). The prognostic variables are the moisture and temperature of the soil layers, water stored on the canopy and snow stored on the ground. Daily surface runoff is computed by the Simple Water Balance (SWB) model (Schaake et al., 1996). The NOAH-LSM computes actual evapotranspiration separately for the following components: Direct evaporation (Eq. 2), evaporation of intercepted water (Eq. 3) and transpiration (Eq. 4).

$$E_{dir} = \left(1-\sigma_f\right) \beta \, E_p \tag{2}$$

$$E_i = \sigma_f \; E_p \left(\frac{W_c}{S}\right)^n \tag{3}$$

$$E_t = \sigma_f \; E_p \; B_c \left[1-\left(\frac{W_c}{S}\right)^n\right] \tag{4}$$

Besides the green vegetation fraction (σ_f), the NOAH-LSM is taking the soil water content (β), the intercepted canopy water content (W_c), the maximum canopy capacity (S) as well as a plant coefficient (B_c) as a function of canopy resistance into account (Chen et al., 1996).

The green vegetation fraction (σ_f) strongly influences simulation results since it acts as a fundamental weighting coefficient of potential evaporation (E_p) within the calculation of all components of evapotranspiration. MM5 uses monthly values of green vegetation fraction (σ_f) (also known as F_{cover}) for each grid cell at the model's spatial resolution in order to take seasonal phenological behaviour of vegetation into account. It is defined as a function of NDVI

$$\sigma_f = \frac{NDVI - NDVI_0}{NDVI_\infty - NDVI_0} \qquad (5)$$

where $NDVI_0$ and $NDVI_\infty$ are the lower and upper 5% of the global NDVI distribution for the whole year and therefore describe the signals from bare soil and not-vegetated areas and dense green vegetation respectively (Chen et al., 1996; Gutman and Ignatov, 1997). Since the $NDVI_\infty$ is likely to reach saturation, this approach tends to overestimate σ_f (Richter and Timmermans, 2009). Uncertainties of NDVI due to soil moisture, soil type and color, dead vegetation and shadow-effects within the plant stand as well as atmospheric effects such as cloud contamination and angular effects of the radiometer field-of-view (FOV) affect satellite-based measurements of the vegetation fraction, making it an unreliable quantity (Bach and Verhoef, 2003; Gutman and Ignatov, 1997; Richter and Timmermans, 2009). Further, the use of the 5th percentile seems arbitrary for global mapping of σ_f since this is only valid for pixels with assumed dense vegetation (Gutman and Ignatov, 1997). The green vegetation fraction concerning this study was gathered by a 5-year time series of NDVI (Chen et al., 1996; Gutman and Ignatov, 1997) from AVHRR (US Geological Survey (USGS)), with a spatial resolution of 10 minutes (18,5 km) and global coverage. It was further generally reduced by 30 percent since it proved to be too high for our simulation area and this reduction helped to improve the simulation of summertime near surface temperature substantially (Pfeiffer and Zängl, 2009).

However, it must be pointed out that this approach was introduced by climatologists with the intention of introducing a simple parameter in climate models for worldwide application since it is gathered from satellite data and therefore avoid complex parameterization of individual plants. Also with respect to computational costs, it is a simple and fast approach to implement seasonal behaviour of vegetation. However, it represents a delicate parameter with a large potential of uncertainty due to its impact on evapotranspiration, which results in errors.

Within E_t, the canopy treatment is an important issue. The canopy resistance (R_c) is formulated as follows in the NOAH-LSM (Eq. 6),

$$R_c = \frac{R_{c\min}}{LAI\ F_1 F_2 F_3 F_4} \qquad (6)$$

where F_4 is the water-stress function with respect to soil moisture while F_1, F_2 and F_3 represent the effects of solar radiation, vapour pressure deficit and air temperature on the canopy resistance. The values of all functions range between 0 and 1; LAI is the leaf area index and $R_{c\min}$ is the minimum canopy resistance which is set to 5000 s m^{-1} for all plants (Jacquemin and Noilhan, 1990; Noilhan and Planton, 1989). The LAI does not change with season and for all land use classes of the NOAH-LSM has a value of 4.0. The temperature-stress function is the same for all plants, the optimum transpiration temperature being parameterized with 298 K (Chen and Dudhia, 2001a). The dynamic function of water-stress (F_4) is a factor for the availability of soil moisture, however neglecting plant specific parameters (Eq. 7).

$$F_4 = \sum_{i=1}^{3} \frac{(\Theta_i - \Theta_w) d_{zi}}{(\Theta_{ref} - \Theta_w)(d_{z1} + d_{z2})} \qquad (7)$$

It is a function of volumetric soil moisture content (Θ) and the soil specific parameters of field capacity (Θ_{ref}) and the wilting point (Θ_w) for the upper three soil layers integrated in the rooted zone (Chen and Dudhia, 2001a), parameterized as percentage values of soil moisture.

4-2-2 PROMET

PROMET was developed for hydrological river catchment studies on the local and regional scale. It describes processes at the land surface physically based with high detail and complexity using several sub-modules (Figure 5). It is conserving mass and energy and closes the energy balance at the land surface. It was applied in this study with an hourly temporal and 1km spatial resolution. An extensive model description can be found in Mauser and Bach (2009).

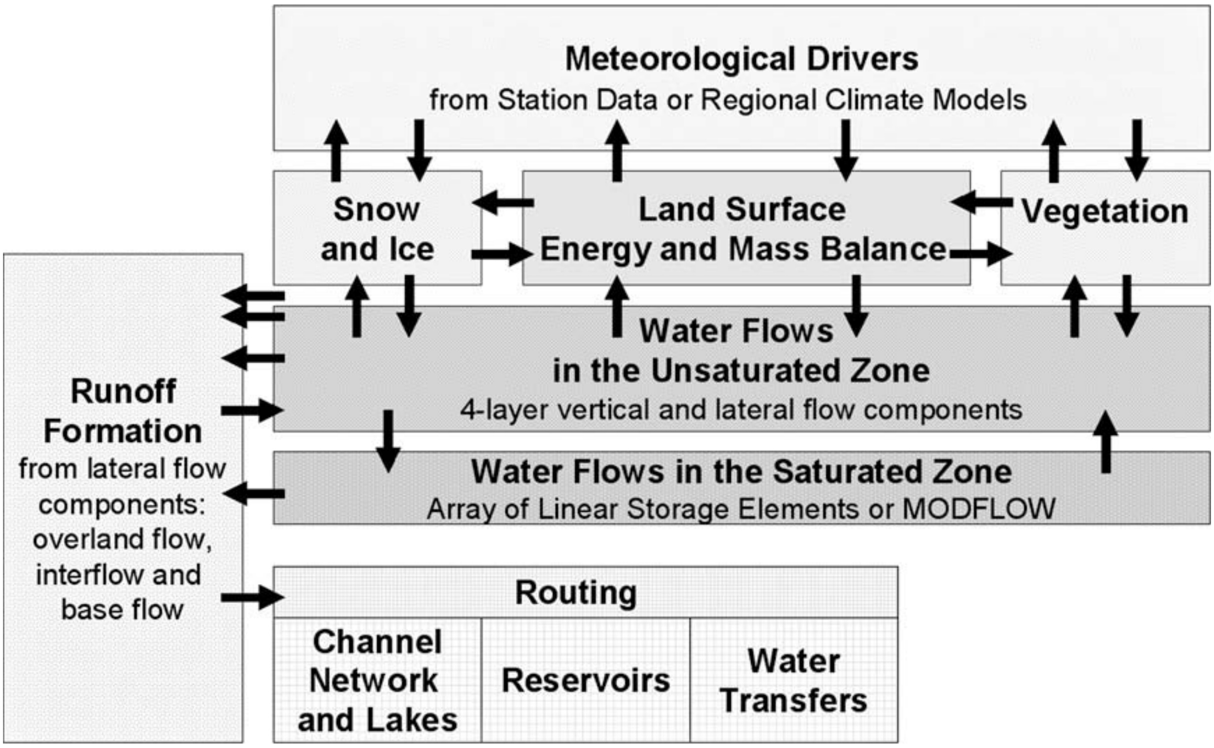

Figure 5: Model components of PROMET

PROMET has already been used in several small and large scale watersheds ranging from a few hundred km² to app. 1 mil. km² and has been extensively validated in different regions in the world (Hank, 2008; Koch et al., 2011; Loew, 2008; Loew et al., 2009; Ludwig and Mauser, 2000; Ludwig et al., 2003a; Ludwig et al., 2003b; Marke et al., 2011a; Mauser and Schädlich, 1998; Mauser and Bach, 2009; Muerth, 2008; Prasch et al., 2006; Prasch et al., 2011; Strasser, 1998; Strasser and Mauser, 2001; Strasser et al., 2007; Weber et al., 2010).

Actual evapotranspiration within the vegetation component of PROMET is simulated using the Penman-Monteith equation (Mauser and Schädlich, 1998; Monteith, 1965; Monteith and Unsworth, 2008), closing the energy balance iteratively (Mauser and Bach, 2009). The water pathway via the soil through the roots into the leaf and passing via the stomata into the laminar and finally the turbulent atmosphere, is driven by the potential difference of water vapour pressure between the soil and the atmosphere, assuming that the atmospheric suction is limited by a number of resistances similar to electrical conductivity (Monteith and Unsworth, 2008). The canopy resistance is calculated for individual plant types following an approach by Baldochi et al (1987) and Jarvis (1976). The stomata resistance (R_c) is a function of radiation (PAR), temperature (F_1), ambient humidity (F_2), CO2 in the atmosphere (assumed to be constant) and the leaf water potential (F_3) (Jarvis and Morison, 1981) (Eq. 8).

$$R_c = \frac{R_{c\min}(PAR)}{F_1 F_2 F_3} \quad (8)$$

PAR is calculated according to the fractions of sunlit and shaded leaf area and the PAR flux densities on the respective leaves (Baldocchi et al., 1987). The relation of temperature, humidity deficit and leaf water potential to the stomata resistance is described with F_1, F_2 and F_3 following Jarvis (1976), returning values between 0 and 1. An increase in temperature beyond a plant specific optimum results in an increase of stomata resistance since the plant's stomata will close in order to protect itself against dehydration, which results in a decrease of transpiration. The conductivity is reduced to the minimum stomata conductivity, which is the conductivity of the cuticle.

The inhibition due to water stress (Eq. 9) is quantified in PROMET in terms of leaf water potential, which depends in a plant-specific way to the soil water potential (Ψ_s) within the rooted soil layers.

$$F_3 = ((\Psi_s + R_r) - \Psi_0) * a\Psi + b\Psi \quad (9)$$

The stomatal conductance shows no dependence on leaf water potential below a plant specific threshold (ψ_0) of suction and an approximately linear plant specific decrease beyond (Baldocchi et al., 1987), and takes the resistance of the transition from the soil to the root (R_r) into account (Biscoe et al., 1976). The parameters R_r , Ψ_0, $a\Psi$ and $b\Psi$ are parameterized for each plant type in PROMET. The soil water potential is a function of soil type and soil water content following an approach of Brooks and Corey (1964).

Overall, PROMET includes a detailed soil and plant parameterization in order to consider the complexity of the physical description of the land surface processes. The parameterization of a wide range of vegetation types in PROMET is taken from literature and remote sensing data (Bach, 1995; Mauser and Bach, 2009). Typical daily change of the plant parameters LAI, albedo, root depth and plant height were taken from the analysis of time series of LANDSAT images in Southern Germany in combination with extensive field measurements on typical plant stands (Mauser and Bach, 2009) thereby taking phenological behaviour of different stands and spatial heterogeneity into account (Zabel et al., 2010).

5 Coupling approaches

Since NOAH-LSM is an integral part of MM5 it is required within the RCM to model the land surface processes at the same temporal and spatial resolution as the atmospheric model components of MM5.

PROMET differs from MM5 both in temporal and spatial resolution. In order to interactively couple PROMET with MM5, the coarse meteorological data provided by MM5 (45x45 km) has to be downscaled to the higher resolution of the land surface model (1x1 km). Besides, the surface fluxes simulated by PROMET at a resolution of 1 km have to be upscaled to the MM5 model resolution. This is done by applying the scaling tool SCALMET (**Scal**ing **Met**eorological variables) (Marke, 2008; Marke et al., 2011a). In the context of downscaling meteorological fields, SCALMET has been successfully used with different offline coupled applications under a variety of hydro-meteorological boundary conditions e.g. in the Upper Danube Watershed in Europe (Marke, 2008; Marke et al., 2011a; Marke et al., 2011b), in the Upper Brahmaputra Watershed in Asia (Prasch et al., 2011) or in the Gâtineau watershed in the US and Canada (Ludwig et al., 2009). In the framework of these studies, past as well as possible future hydrological scenarios have been simulated using PROMET with the meteorological drivers provided by different regional climate models (MM5, REMO, CLM, CRCM). The adjustable simulation time step within PROMET, which also constitutes the exchange time step between PROMET and MM5, is set to 9 minutes in the current study. This allows PROMET to run synchronously with MM5, which uses a internal time-step of 135 seconds. The statistical downscaling can either be used with regression based approaches (Daly et al., 2002) or empirical gradients (Liston and Elder, 2006), using elevation-dependencies in order to scale the meteorological data to the fine resolution grid.

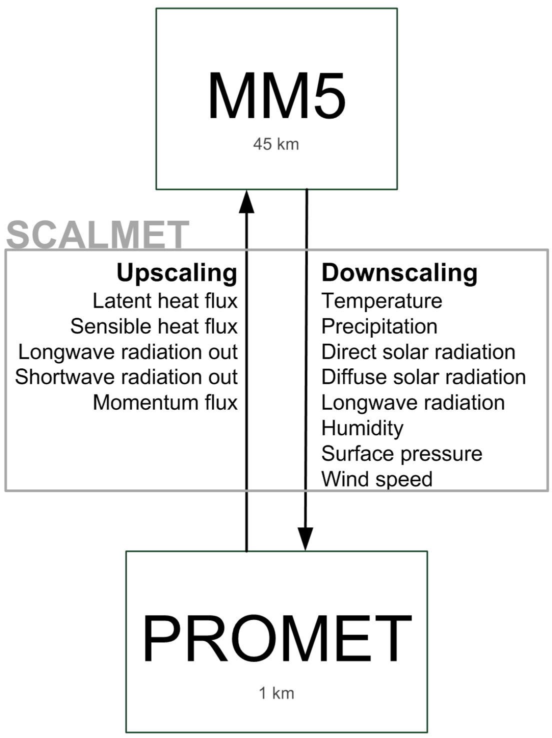

Figure 6: The model setup when interactive coupling MM5 and PROMET using the scaling interface SCALMET.

In addition to the offline downscaling approach in SCALMET, a 2-way (bidirectional) and therefore interactive coupling mode was implemented in SCALMET allowing for a linear upscaling of the scalar surface fluxes (see Figure 6). In order to close the energy balance in the interactive coupled land-atmosphere system, the downscaling as well as the upscaling approach strictly conserves mass and energy within the scaling processes in SCALMET for each variable. Hence, no bias correction is carried out in the framework of the model runs presented in this study. Therefore, any bias of the RCM is inevitably inherited by the LSM and vice versa.

The interactions between the land surface and the atmosphere are based on the exchange of latent and sensible heat, short and longwave radiation as well as momentum (Campbell and Norman, 2000). The energy balance of the overall atmosphere-land-system is given in Eq. 10 (Dingman, 2002).

$$\downarrow R_{short} + \downarrow R_{long} = \uparrow H_{latent} + \uparrow H_{sensible} + \uparrow R_{long} + \uparrow R_{short} + \downarrow H_{ground} \qquad (10)$$

Where R_{short} and R_{long} are the incoming shortwave and longwave radiation that are partitioned into the latent heat flux (H_{latent}), the sensible heatflux ($H_{sensible}$) and the shortwave and longwave outgoing radiation (R_{short} and R_{long}) and the ground flux (H_{ground}).

6 Results and discussion

6.1 Comparing model evapotranspiration with equal meteorological drivers

Figure 7 shows the mean annual evapotranspiration from 1996-1999 simulated by the NOAH-LSM (left) and by PROMET-offline (right).

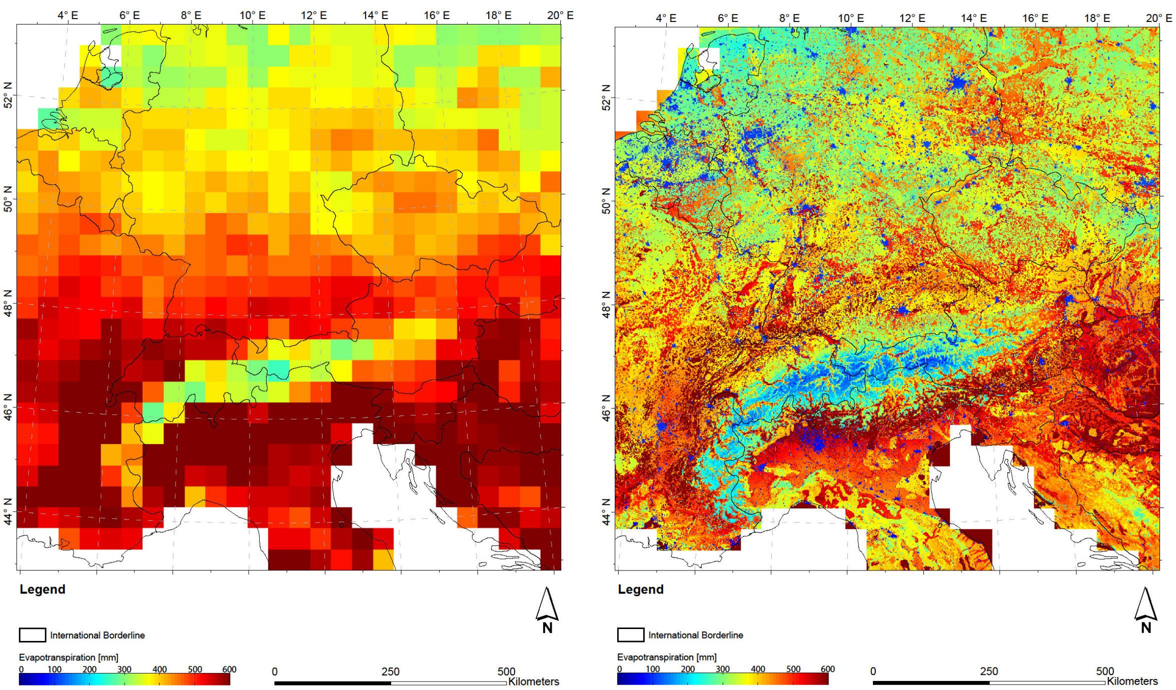

Figure 7: Mean annual evapotranspiration of NOAH-LSM (left) and PROMET-offline (right)

Overall, the NOAH-LSM simulates a mean annual evapotranspiration of 469 mm and PROMET-offline 397 mm. The remarkable mean difference of more than 70 mm for the area average which is more than 17 % is diversely spatially distributed and has several reasons we further aim to investigate. Basically, both models show a north to south gradient of evapotranspiration and lower values in the alpine region, which corresponds to the prevailing climate conditions. The most obvious difference is the spatial heterogeneity related to the spatial resolution applied to each model. The PROMET-offline evapotranspiration allows for recognizing small-scale spatial patterns such as alpine valleys with high contrasts to its surroundings and forested areas with high evapotranspiration as can be found e.g. in the Black Forest (approx. 48.5°N 8.3°E). While the PROMET land-use data set includes a number of impervious surfaces (such as residential or industrial areas and rocks) that do not contribute to transpiration and therefore reduce mean annual evapotranspiration, the NOAH underlying land-use data set accounts only for a small number of land-use classes and mainly implements cropland in the model domain (see Figure 4). The effect of different land-uses and impervious surfaces in PROMET becomes especially apparent in large urban areas such as Berlin or the extended Ruhr region as well as in rocky alpine areas (see Figure 7). In order to compare the model results on the same spatial scale, we aggregated the PROMET-offline result to the spatial resolution of 45 x 45 km and finally subtracted it from the NOAH evapotranspiration (Figure 8).

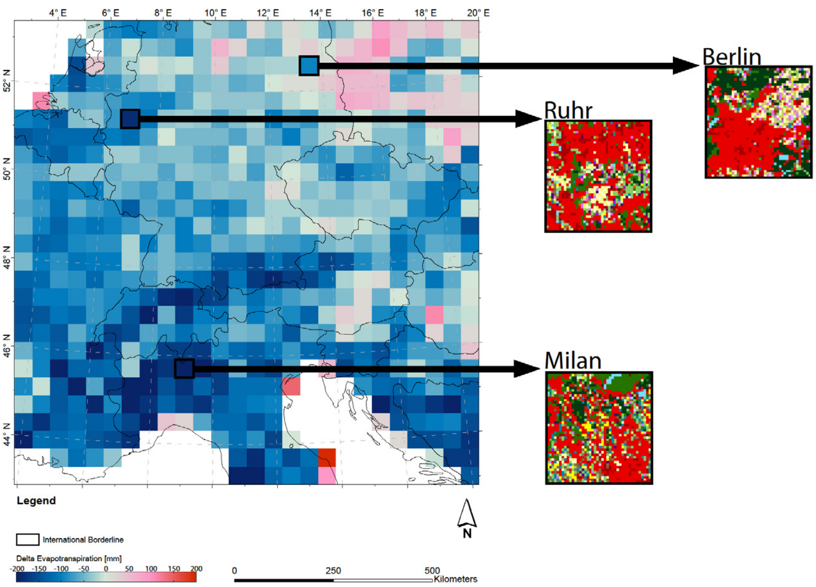

Figure 8: Difference plot of mean annual evapotranspiration of PROMET-offline and NOAH-LSM exemplary compared to 1 km² land use (legend see Figure 4) for the Berlin, Ruhr and Milan pixel (red indicates urban areas).

The overall mean annual evapotranspiration is lower in the PROMET-offline simulation. Pixels with high percentage of impervious surfaces in PROMET such as Berlin (43 %), the Ruhr region (55 %) and Milan (37 %) show the highest differences of evapotranspiration (see Figure 8) while the NOAH-LSM is parameterized with cropland in all of those pixels (see Figure 4). The simulated mean annual evapotranspiration for the Berlin pixels is 95 mm less per year in the PROMET-offline simulation (260 mm) than in the NOAH simulation (355 mm), 183 mm less for the corresponding Ruhr pixels (NOAH: 405 mm; PROMET: 222 mm) and even 283 mm less in the Milan pixels (NOAH: 707 mm; PROMET: 424 mm), which are the pixels with the largest difference.

Caused by the impervious surfaces in PROMET, annual transpiration contributes 56 % to evapotranspiration for the Milan pixels, 36 % for the Berlin pixels and 30 % for the pixels of the Ruhr region.

Additionally, The effect of the different land-uses on simulated evapotranspiration can be investigated by comparing the temporal mean monthly behaviour of evapotranspiration (1996 - 1999) of the NOAH-LSM and the PROMET-offline simulations.

Figure 9 takes a closer look at Milan and shows monthly NOAH-LSM and PROMET-offline evapotranspiration exemplary for the 45x45 km Milan pixel, which contains 2025 different PROMET pixels. The PROMET land-use data for the 45x45 km MM5 Milan pixel contains 40 % residential and industrial pixels, 30 % forested areas and 30 % arable land within which 32 % are intensive grassland, 26 % are maize and silage (each 13 %) and 14 % are set-aside. The land-use data was compiled from CORINE 2000 data combined with MERIS NDVI and EUROSTAT statistical data (Zabel et al., 2010). The PROMET-offline results are displayed with and without the impervious PROMET pixels within the Milan MM5 pixel in Figure 9.

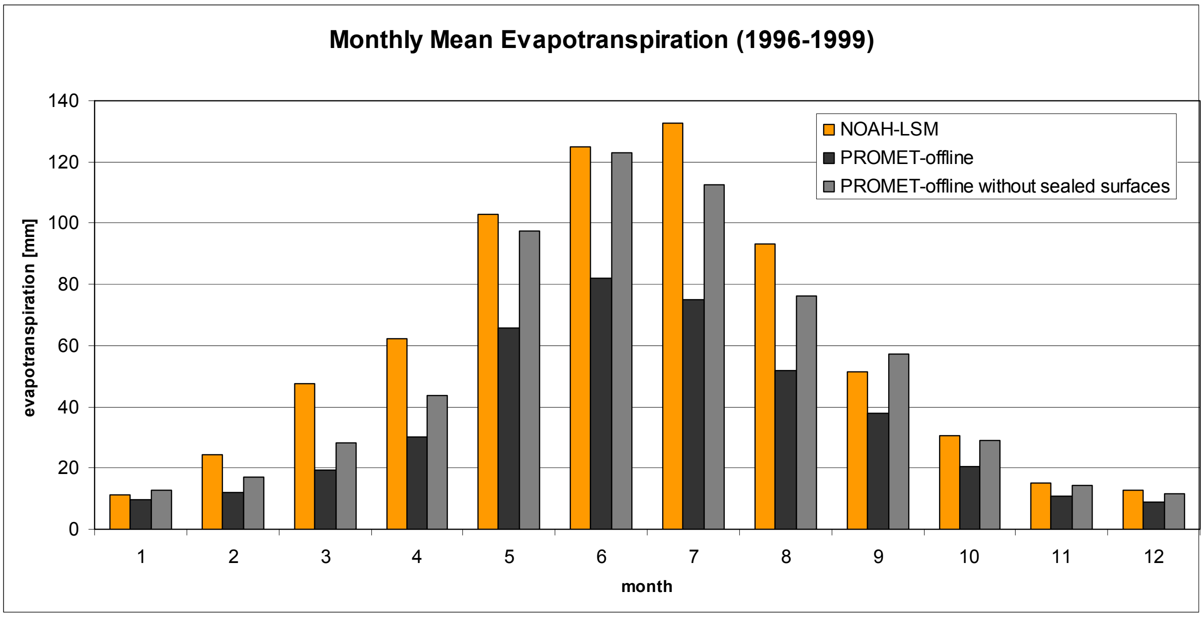

Figure 9: Monthly mean evapotranspiration from 1996 - 1999 for the Milan Pixel of the NOAH-LSM and all corresponding PROMET-offline pixels respectively masked without impervious surfaces, only accounting vegetated pixels.

The prominent role of impervious surfaces in producing the average evapotranspiration can clearly be seen during the summer months, when NOAH-LSM and PROMET-offline evapotranspiration differ largely when looking at the average evapotranspiration of all PROMET pixels of Milan. This difference in summer almost disappears when excluding the impervious pixels from the analysis and only taking the vegetated PROMET pixels into account. The annual difference in evapotranspiration between NOAH-LSM and PROMET-offline is then reduced from about 200 mm to 86 mm. It is also remarkable that the largest differences, neglecting impervious surfaces within the PROMET-offline simulation, occur in the spring months (March, April) and in summer (July, August).

While the NOAH-LSM uses monthly variations of the green vegetation fraction (σ_f) in order to take seasonal behaviour of vegetation into account, PROMET uses daily courses of LAI, plant-height, albedo and root depth for each of its vegetation classes. This results in a heterogeneous behaviour of evapotranspiration in the PROMET-offline simulation in spring. In Figure 9, PROMET-offline evapotranspiration in April is a mixture of large values of the developing cereal plants and small values for bare soil of open maize fields (which do not exist in the NOAH-LSM). Both in spring and summer, monthly mean evapotranspiration differs largely while in winter, differences are small since evapotranspiration is mainly energy and not land-use driven (Figure 9).

Figure 10 shows the comparison of the monthly development of the green vegetation fraction for the Milan pixel in the NOAH-LSM with the daily development of LAI for the most important land use classes for the corresponding PROMET pixels neglecting impervious surfaces. While cereals are harvested in the late summer and grassland is mowed three times a year in the PROMET parameterization, harvest times are not considered directly in the NOAH plant parameterization. Another prominent gap between the two model parameterizations can be recognized in April (Figure 10).

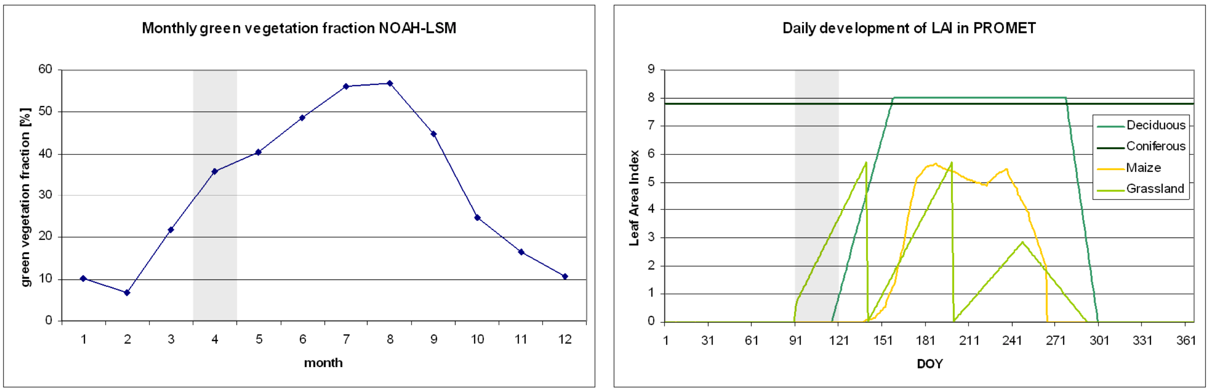

Figure 10: NOAH-LSM development of the green vegetation fraction of the considered Pixel in the Po-valley and daily LAI development for deciduous forest, maize and grassland in PROMET.

The monthly green vegetation fraction shows values of almost 40 % in April which means that 40 % of potential evaporation is possible in the NOAH-LSM. However, at the same time, the PROMET phenological development of deciduous forest and maize has not yet started and thus only the grassland and coniferous forested areas are contributing to transpiration. As a result, the PROMET's monthly share of transpiration to evapotranspiration is about 30 % regarding the vegetated Milan pixels in April.

In the summer months, vegetated stands are fully developed in both models but still, evapotranspiration rates for not impervious surfaces of PROMET are below those of the NOAH-LSM which is most likely due to water stress in the PROMET-offline simulation that reduces summer plant transpiration rates. Since the water stress functions included in both models are not comparable due to different model approaches and different impacts on transpiration, Figure 11 compares the daily course of simulated soil moisture between both models for the third soil layer representing the Milan pixel in the NOAH-LSM. The PROMET-offline soil moisture is exemplarily shown for a pixel vegetated with maize and parameterized with the soil type 'loamy clay' in the 3rd soil layer which occurs most frequently (55 %) within the Milan area pixels, while MM5 is parameterized with soil type clay. The layer thickness reaches from 1 m to 2 m from the land surface in the NOAH-LSM and reaches from 0.5 m to 1.5 m in PROMET. Soil properties describing water retention of the 3rd soil layer are most important in providing water for plant transpiration since maize is parameterized with a root fraction of 60 % within the 3rd soil layer in PROMET. The most important soil parameters within the NOAH-LSM that are necessary to determine water availability in terms of plant transpiration, are the maximum soil moisture (46.8 Vol-%. for the Milan pixel), the field capacity (41.2 Vol-%. soil moisture) and the wilting point (13.8 Vol-%. soil moisture).

Both models show a similar behaviour of soil moisture in the winter months. During the Mediterranean summer months, the soil moisture decreases in the NOAH simulation while it stops decreasing in the PROMET simulation reaching a threshold of 29 Vol-%. soil moisture each summer (see Figure 11). This is due to the increasing soil suction in the “loamy clay” pixel and the reaction of maize to soil moisture deficit. Maize in PROMET is parameterized to react quite sensitively to increasing soil suction and starts restricting evapotranspiration at levels of soil suction of 0.8 MPa and completely closes stomata at 1.2 MPa, which is reached in the “loamy clay” soil at soil moisture levels of app. 29 Vol-%. This has a strong impact on the transpiration rate in the summer (see Figure 12). The decrease in soil moisture within the NOAH simulation shows that soil water from the 3rd layer is still used for transpiration during the summer months, since the wilting point is parameterized with 13.8 Vol-% soil moisture. This value seems unusually low for an assumed clay soil in the MM5 soil dataset.

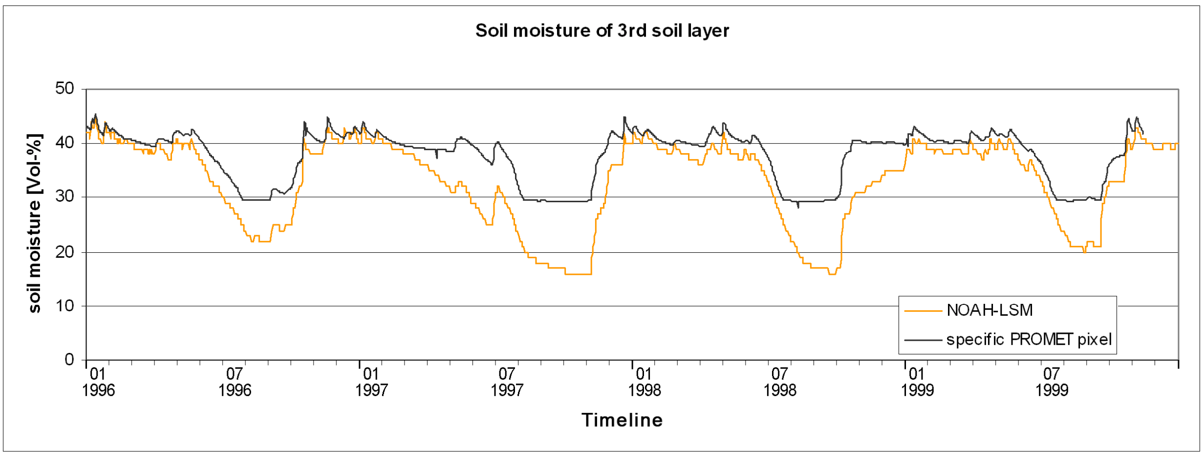

Figure 11: Daily soil moisture (1996-1999) of the 3rd soil layer simulated by the NOAH-LSM for the Milan 45 km² pixel and by PROMET-offline exemplarily for one 1 km² pixel inside the Milan area with land-use maize and soil type 'loamy clay' in the 3rd soil layer.

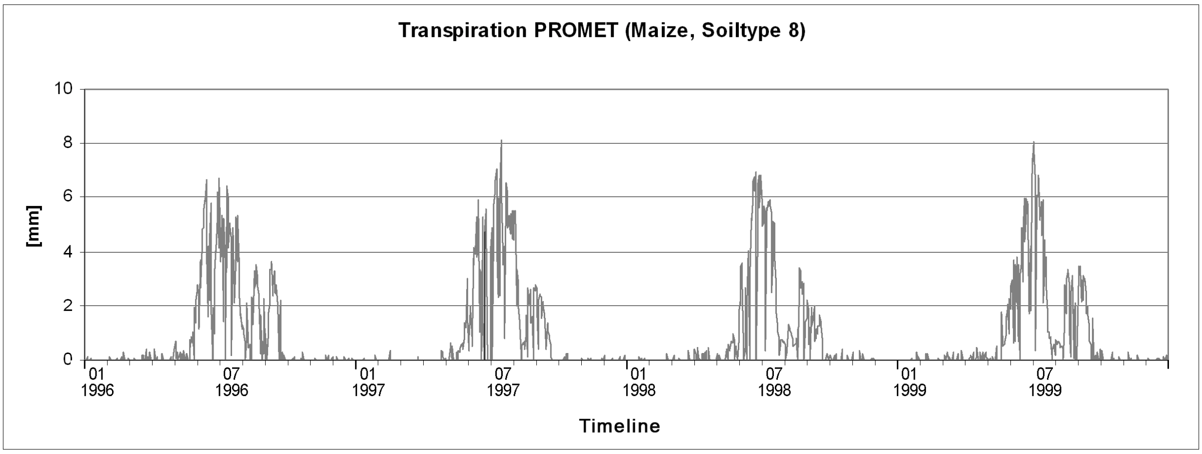

Figure 12: Daily transpiration (1996-1999) simulated by PROMET-offline exemplarily for one 1 km² pixel with land-use maize and soil type 'loamy clay' in the 3rd soil layer.

The development of the pF-value for the same PROMET sample-pixel is shown in Figure 13 in order to proof that the reduced transpiration is due to a limitation in the soil water and not due to other limitations e.g. solar radiation. It is calculated as in PROMET after an approach of Brooks and Corey (1964) calculating the matrix potential // soil water potential (Ψ_s) as the following:

$$\Psi_s = \Psi_1 \cdot S^{-1/m} \tag{11}$$

where Ψ_1 is the air entry tension (bubbling pressure head), S is the saturation of the effective pore space with water and m is the pore-size distribution index, which are all parameters also available within the soil parameterization of PROMET.

Figure 13 demonstrates that the inhibition of transpiration is due to the increasing soil water potential in the 3rd soil layer. Maize is unable to suck more water out of the soil since the permanent wilting point is reached at the pF-value of about 4.2 when the soil moisture reaches less than 29 Vol-%.

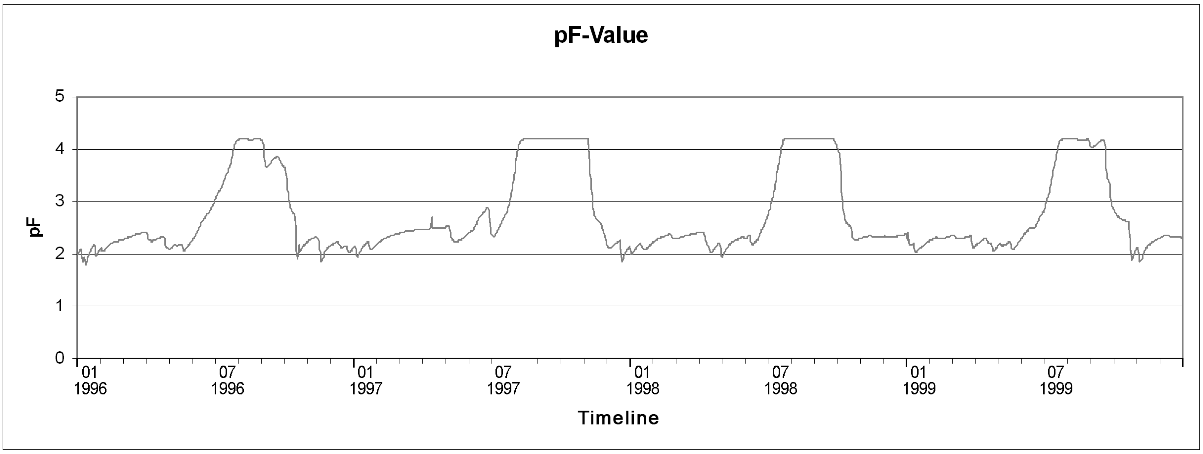

Figure 13: Daily pF-value (1996-1999) simulated by PROMET-offline exemplarily for one 1 km² pixel with land-use maize and soil type 'loamy clay' in the 3rd soil layer.

6-2 Quantification of feedbacks between the land surface and the atmosphere

The simulated evapotranspiration between the NOAH-LSM and PROMET-offline, as showed differ both in spatial and temporal manner. Finally, the impact of these differences on feedback effects between the land surface and the atmosphere are investigated. Thus, the inconsistencies within the offline coupling approach due to neglecting the feedbacks are quantified. Therefore, PROMET is now interactively coupled with MM5 thus substituting the NOAH-LSM and finally providing the lower boundary conditions for the MM5 atmosphere (Figure 2 and Section 5). Energy conservation is guaranteed within the interactively coupled system. Since feedbacks mutually affect the atmosphere and the land surface in a complex way, they cannot be separated. This chapter first describes the impact of feedbacks on the MM5 atmosphere in terms of temperature and precipitation. Finally, the impact of feedbacks on the interactively coupled PROMET (PROMET-interact) evapotranspiration is investigated.

6-2-1 Air temperature

Figure 14 compares the mean annual near surface air temperature between the MM5 simulation either using the NOAH-LSM or PROMET-interact. While the mean temperature over the simulation area is 9.4° C in the MM5-PROMET-interact simulation, it is 8.5° C in the MM5-NOAH simulation. Despite the replacement of the NOAH-LSM, still a similar temperature can be reproduced within the MM5-PROMET-interact simulation with regional differences (Figure 14). The tendency of less transpiration in the PROMET-offline simulations in comparison to the NOAH-LSM may be a major reason for overall higher air temperature in the MM5-PROMET-interact simulation than in the MM5-NOAH one. The mutually dependent effect of less transpiration, due to impervious surfaces and higher near surface air temperature, can clearly be seen in the pixels of Berlin, the Ruhr as well as the Milan pixel (Figure 14). Here, feedbacks with the PROMET-interact land surface result in higher temperatures in the MM5 atmospheric model by up to 2.4 K (in the Ruhr region), which can also be seen in the subtraction image in Figure 14.

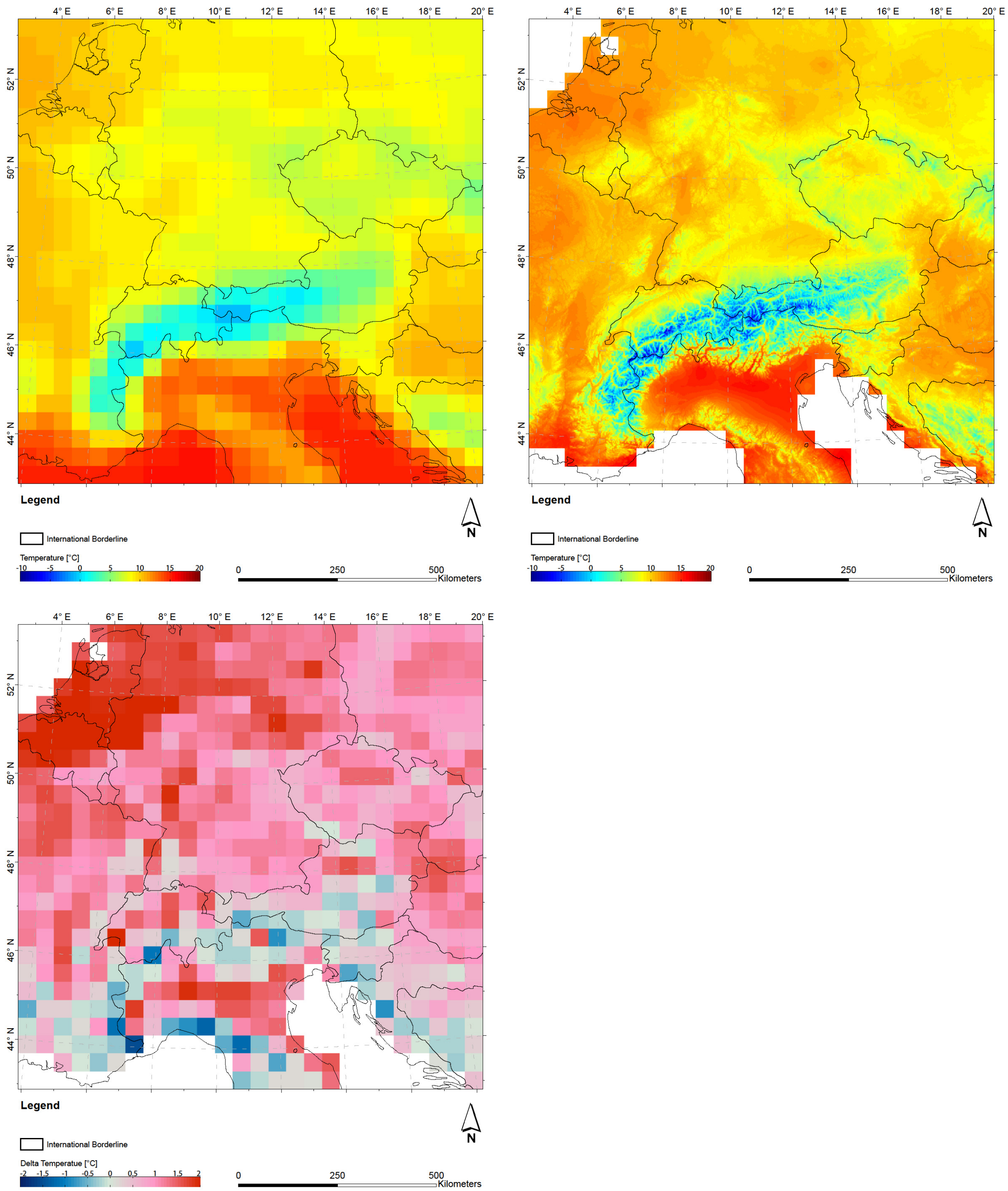

Figure 14: Mean annual near surface air temperature [°C] (01.01.1996 - 31.12.1999) of MM5 simulations, using the NOAH-LSM at a spatial resolution of 45 km (upper left) and MM5 simulations, using PROMET-interact at a spatial resolution of 1 km and finally downscaled with SCALMET (upper right). Subtraction image of MM5-PROMET-interact and MM5-NOAH simulations (lower left).

The mean monthly temporal behaviour exemplarily shown for the Milan pixel in Figure 15 shows that the annual course can be reproduced in the MM5-PROMET-interact simulations. However, strong feedbacks by using PROMET-interact affect the near surface air temperature for the Milan pixels especially in summer. Maximum differences (3.3° K) appear in June, while in winter, when energy assumption at the land surface is low, temperature is hardly affected by feedbacks. The Milan pixels annually show a 12 % warmer near surface air temperature (14.2° C) than the MM5-NOAH simulation (12.6° C).

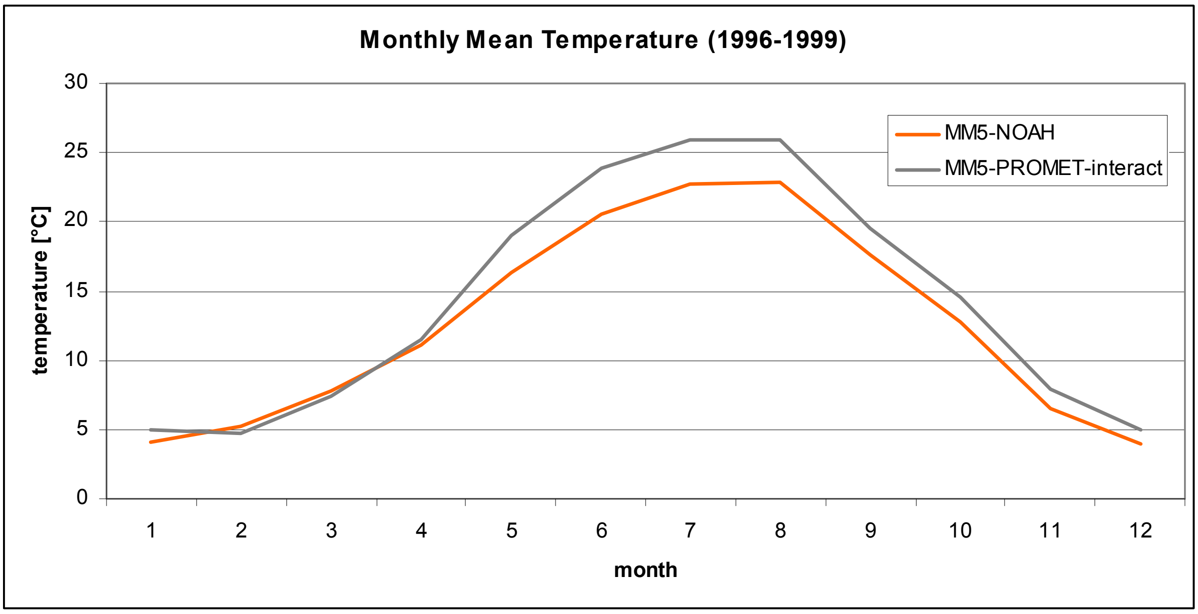

Figure 15: Monthly mean of near surface air temperature [°C] (01.01.1996 - 31.12.1999) of MM5-NOAH simulation and MM5-PROMET-interact simulation for the Milan pixel and the corresponding Milan pixels respectively.

6-2-2 Precipitation

Besides temperature, precipitation is another parameter strongly interacting with the land surface and which has a large impact on LSHMs. Thereby, the changed lower boundary conditions in the PROMET-interact simulation result in less annual precipitation amounts, especially in the Alpine area (see Figure 16). While the annual precipitation amount over the simulation area is 830 mm in the MM5-PROMET-interact simulation, it is 886 mm in the MM5-NOAH simulation.

The spatial patterns of annual precipitation amounts between MM5-NOAH and MM5-PROMET-interact simulations are almost the same. However, total precipitation amounts decrease mostly north and south of the Alps and in the Po-Valley by up to 213 mm (Figure 16).

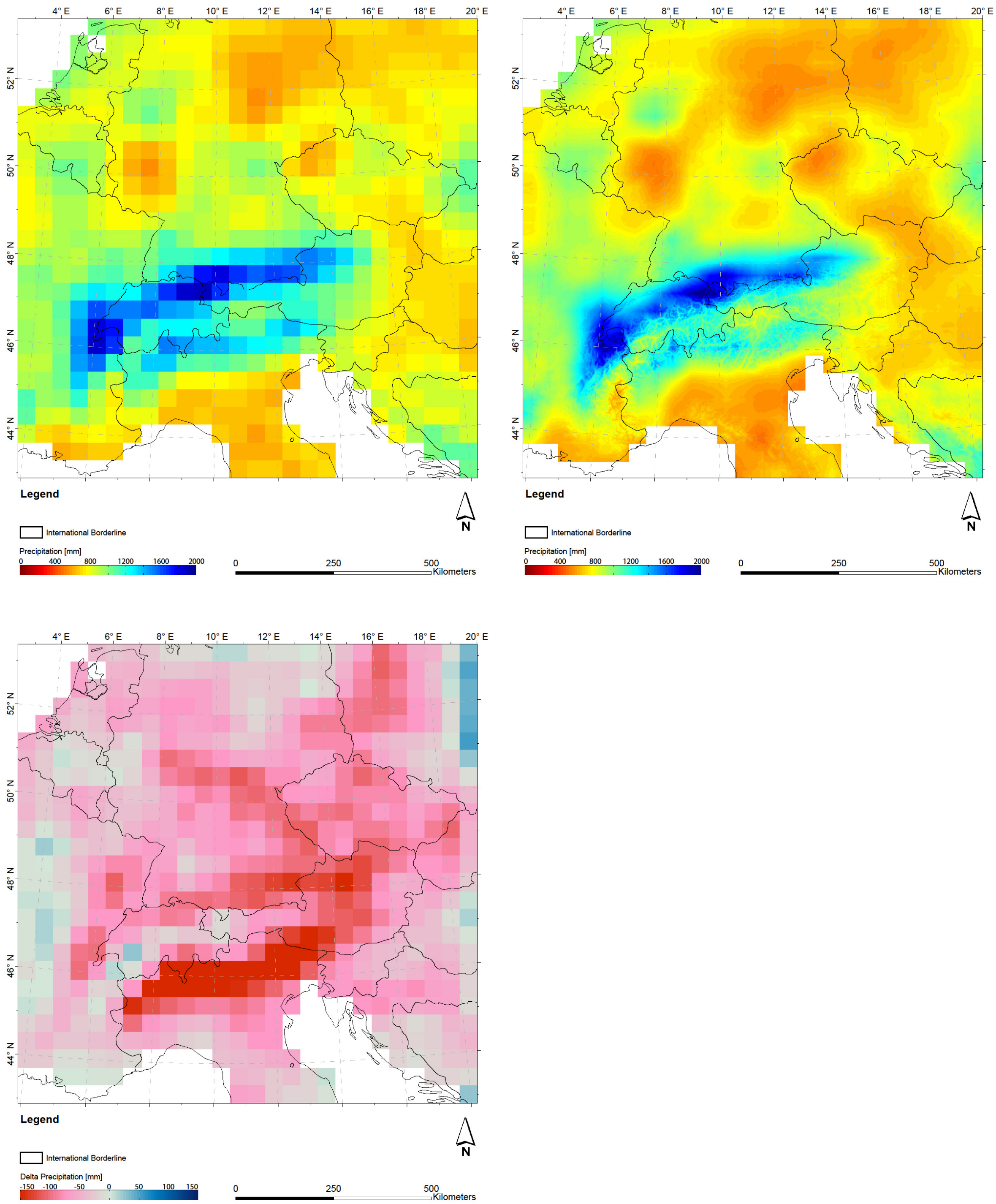

Figure 16: Mean annual precipitation [mm] (01.01.1996 - 31.12.1999) of MM5 simulations, using the NOAH-LSM at a spatial resolution of 45 km (upper left) and MM5 simulations, using PROMET-interact at a spatial resolution of 1 km and finally downscaled with SCALMET (upper right). Subtraction image of MM5-PROMET-interact and MM5-NOAH simulations (lower left).

The monthly behaviour exemplarily shown for the Milan pixel in Figure 17 shows that the annual course can be reproduced in MM5-PROMET-interact simulations. Feedbacks within the MM5-PROMET-interact simulation result in decreased precipitation amounts for the Milan pixels, especially in summer. Maximum differences compared to the MM5-NOAH simulation occur in August, when almost 50 mm less precipitation is simulated by using the PROMET-interact land surface within MM5. The annual precipitation differs concerning the Milan pixels by 164 mm which is about 15 %.

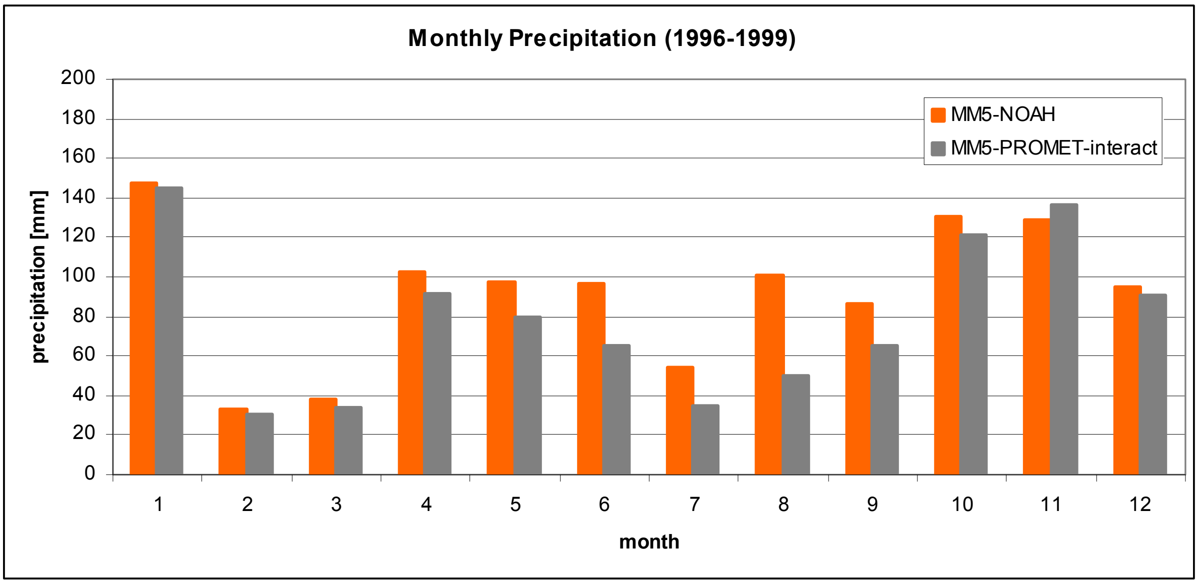

Figure 17: Monthly precipitation amounts [mm] (01.01.1996 - 31.12.1999) of MM5-NOAH simulation and MM5-PROMET-interact simulation for the Milan pixel and the corresponding Milan pixels respectively.

6-2-3 Evapotranspiration

Sect. 6-1 already compared the evapotranspiration between the NOAH-LSM and the PROMET-offline simulation. Now, the impact of the feedbacks by using PROMET-interact as lower boundary conditions for MM5 is investigated. The feedbacks in the MM5-PROMET-interact simulation mutually affect not only the atmosphere conditions, but also the land surface. Figure 18 shows the impact on evapotranspiration, when taking feedbacks between the high resolution PROMET land surface and the MM5 atmosphere into account.

Overall, the annual PROMET-interact evapotranspiration (405 mm) is a little higher than the annual PROMET-offline simulation (397 mm). However, a more detailed spatial analysis shows remarkably smaller annual evapotranspiration rates in the Po-Valley and south of the Alps while annual evapotranspiration rates slightly increased north of the Alps (see Figure 18). The highest impact of the feedbacks on evapotranspiration can be found in the northern part of the Po-Valley, where forested areas (compare with Figure 4) showed high evapotranspiration rates in the PROMET-offline simulation while now, due to feedback mechanism in the PROMET-interact simulation, annual evapotranspiration decreased by about 150 mm. Regions with high vulnerability of plant water-stress, such as the Po-Valley, show the highest differences in simulated evapotranspiration and therefore the highest inconsistencies between the offline and interactive coupling approach.

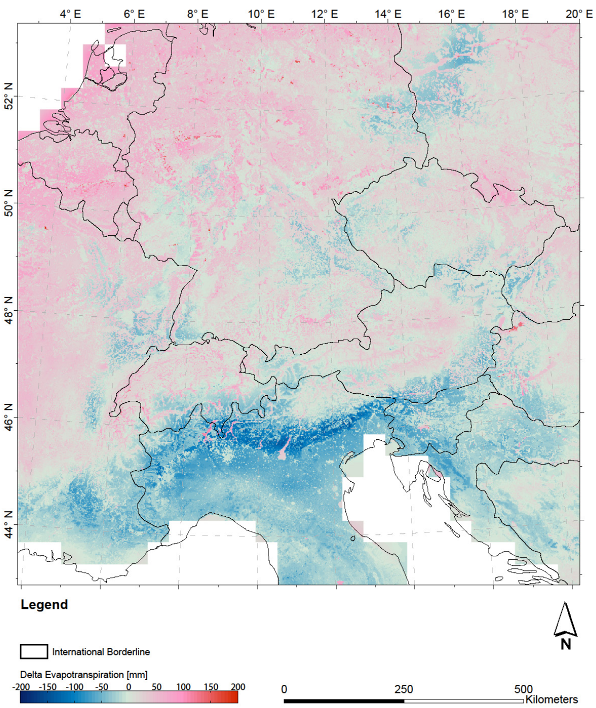

Figure 18: Subtraction image of PROMET-interact and PROEMT-offline simulation for mean annual evapotranspiration (1 x 1 km)

The PROMET-interact evapotranspiration now mutually interacts with the already described temperature and precipitation. Therefore, regional self-amplification effects result in decreased evapotranspiration in regions like the Po-Valley which in turn lead to higher temperature and less precipitation amounts and vice versa.

For the Milan pixels, the annual distinction is approx. 55 mm which is approx. 13 % of the annual evapotranspiration (Figure 19). The inconsistencies of the offline coupling approach are most relevant in the summer months, when PROMET-interact shows drastically decreased evapotranspiration rates e.g. in July of up to 20 mm (27 %), demonstrated exemplarily for the Milan pixels (Figure 19), while in the winter months evapotranspiration is hardly affected by the feedback mechanisms. Evapotranspiration decreased by 30 % from July to September, while at the same time temperature increased by 13 % and precipitation decreased by 37 % (Figure 19, Figure 17, Figure 16).

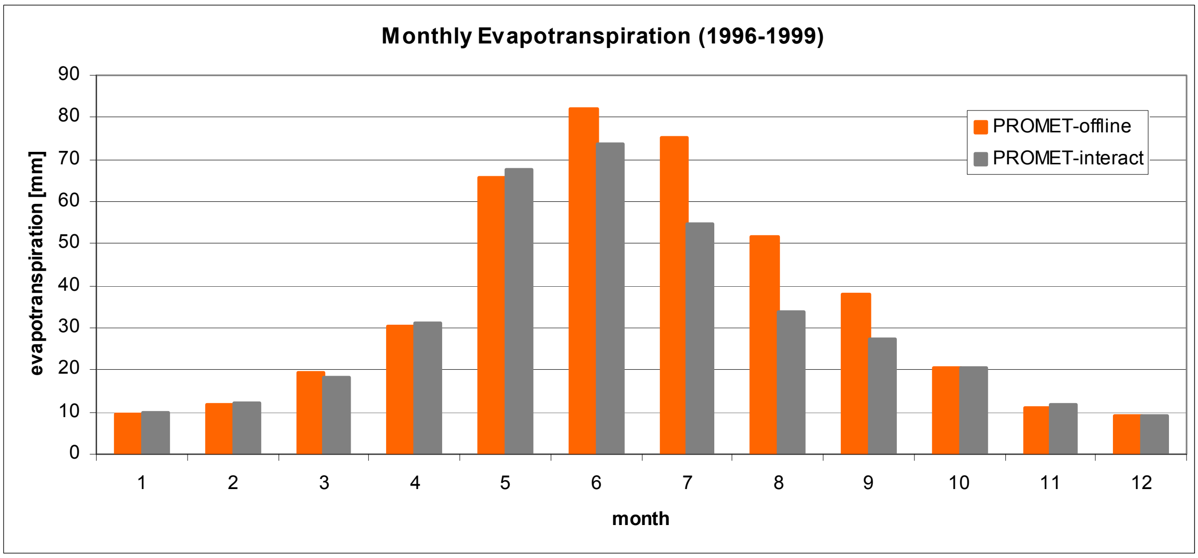

Figure 19: Monthly evapotranspiration rates [mm] (01.01.1996 - 31.12.1999) of MM5-NOAH simulation and MM5-PROMET-interact simulation for the Milan pixels.

While, in the Po-Valley, plant's water suctions already reached the wilting point in PROMET-offline simulations, feedback effects in the PROMET-interact simulations now result in an even higher level of water-stress in the Po-Valley (see Figure 20) which is responsible for the lower transpiration rates. North of the Alps however, transpiration is not or only little limited by water-stress in summer, since still enough water is available for transpiration. Therefore, the feedbacks have predominantly positive effects on transpiration here.

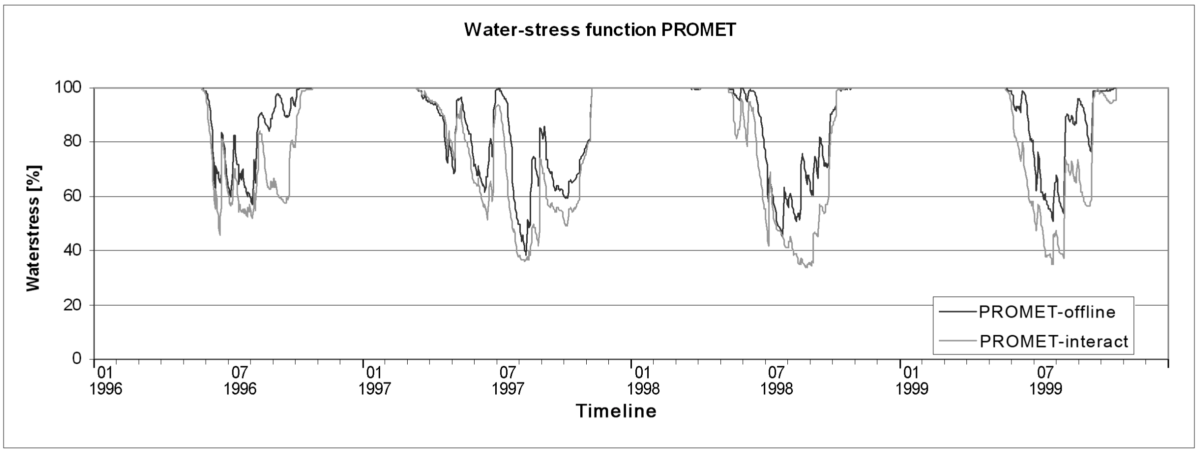

Figure 20: Comparison of water stress function in PROMET-interact and PROMET-offline for the vegetated PROMET pixels of the Milan pixels

7 Conclusions

The study has shown that considerable discrepancies occur between LSMs used within RCMs and downstream climate impact models. Downstream models are driven with RCM data offline and usually focus on specific research questions that the RCM can not or only insufficiently address. The different scales, parameterizations and formulations describing identical land surface processes in the NOAH-LSM used within the RCM MM5 and the downstream hydrological model PROMET, as described in this paper, resulted in considerable differences in evapotranspiration, soil hydraulics and plant water stress.

A finer spatial resolution and therefore a more heterogeneous land surface in PROMET, including impervious surfaces, had a strong hydrological impact on evapotranspiration while the NOAH-LSM assumes the land surface to rather homogeneously consist of arable land which resulted in lower evapotranspiration rates in the PROMET-offline simulation.

The role of plant parameterization in terms of phenological behaviour due to different model assumptions resulted in a temporal delay of PROMET-offline evapotranspiration in spring for the Po-Valley, when compared to the NOAH evapotranspiration. The NOAH-LSM uses simplified parameters like the vegetation fraction with a high degree of uncertainty strongly affecting evapotranspiration. It is not designed to take important aspects of water-stress and plant specific transpiration into account. PROMET, on the other hand uses a large amount of plant and crop dependent parameters resulting in a spatially and temporally higher resolution.

The more comprehensive physical model approaches in terms of the soil and canopy treatment within PROMET resulted in less transpiration than in the NOAH-LSM due to more water-stress in PROMET-offline caused by less soil moisture availability, in particular in the Mediterranean marked Po-Valley.

By coupling of a RCM with a downstream impact model offline, inconsistencies in the coupling approach occur, due to the use of totally different land surfaces within the model chain. Thereby, offline coupling with downstream impact models is neglecting feedback effects between the downstream model and the atmosphere model. Nevertheless, the land surface hydrology strongly interacts with the atmosphere. Therefore, we developed a consistent coupling approach between a RCM and a hydrological downstream climate impact model by interactively coupling the hydrological model PROMET with the MM5 atmosphere. Thus, PROMET substitutes the NOAH-LSM and further provides the lower boundary conditions for the MM5 atmosphere. Consequently, feedback effects between the high spatial resolution hydrological land surface model PROMET and the coarse resolution atmospheric part of MM5 are taken into account. Thereby, the scaling interface SCALMET closes the scale gap between the models and ensures energy conservation within the down- and the upscaling of linear and non-linear energy fluxes.

Despite the replacement of the NOAH-LSM with PROMET, still a similar climate could be reproduced for a 4-year simulation period, showing similar annual values and a similar annual course of monthly mean values for temperature, precipitation and evapotranspiration. However, feedback effects altered precipitation, temperature and evapotranspiration with different regional and temporal behaviour. While annual near surface air temperature mainly increased, annual precipitation amounts mainly decreased for the simulation area. Large differences in annual temperature of more than 2 K could be found especially in regions with a high proportion of impervious surfaces in the PROMET land surface like the Ruhr region. Precipitation amounts mostly decreased in the southern alpine area with a maximum decrease by more than 200 mm. The impact of feedbacks due to the use of PROMET-interact within MM5 on temperature and precipitation were low and negligible in winter but considerably high in the summer months, when energy conversion on the land surface is high and therefore the energy fluxes on the land surface strongly interact with the atmosphere then, finally resulting in greater feedbacks.

The inconsistencies on the simulations of evapotranspiration by using the PROMET-offline approach were investigated by comparing PROMET-offline and PROMET-interact. Inconsistencies were low in the winter months and when regarding averages of the entire simulation area and average annual values. However, inconsistencies were increasing, when getting closer both in temporal and spatial analysis. Evapotranspiration decreased by 30 % from July to September in the Po-Valley, exemplarily shown for the Milan region, while at the same time temperature increased by 13 % and precipitation decreased by 37 %. Regions with a high vulnerability of plant water-stress in summer, such as the Po-Valley, show the highest differences in simulated evapotranspiration and therefore the highest interaction between PROMET and MM5.

As shown, less transpiration in the Po-Valley within the PROMET-offline transpiration in comparison to the NOAH-LSM resulted in higher near surface air temperature and less precipitation when consistently driving the feedbacks with PROMET, which mutually affect the land surface in terms of less evapotranspiration, due to a more detailed description of soil-water and plant processes, and a higher spatial resolution including more land cover types within the PROMET land surface.

The interactively coupling approach requires a large amount of computational resources since it is more extensive than the offline coupled modelling approach due to a higher spatial resolution of the land surface at continental scale and a more complex formulation of land surface processes. The parameterization of the vegetation and soil state therefore requires a larger number of parameters at high spatial resolution on continental scale, which often is difficult due to a lack of adequate datasets. Feedbacks between the RCM and its global forcing on the lateral boundaries are not yet taken into account unless they are another inconsistency within the entire model chain.

Further studies will compare the offline and interactive coupling approach also in terms of radiation and other processes affected by feedbacks. Further, simulation results will be compared with observation data for annual, monthly, and diurnal time series.

8. Acknowledgements

The research described in this paper was carried out at the Department of Geography of the Ludwig Maximilians Universität in Munich, Germany as part of the GLOWA-Danube project, which was funded by BMBF from 2000 to 2010. The support is gratefully acknowledged.

9. References

Bach, H., and Verhoef, W.: Sensitivity studies on the effect of surface soil moisture on canopy reflectance using the radiative transfer model GeoSAIL, Igarss 2003: Ieee International Geoscience and Remote Sensing Symposium, Vols I - Vii, Proceedings, 1679-1681, 2003.

Baldocchi, D. D., Hicks, B. B., and Camara, P.: A canopy stomatal resistance model for gaseous deposition to vegetated surfaces, Atmospheric Environment (1967), 21, 91-101, Doi: 10.1016/0004-6981(87)90274-5, 1987.

Bharati, L., Rodgers, C., Erdenberger, T., Plotnikova, M., Shumilov, S., Vlek, P., and Martin, N.: Integration of economic and hydrologic models: Exploring conjunctive irrigation water use strategies in the Volta Basin, Agricultural Water Management, 95, 925-936, DOI: 10.1016/j.agwat.2008.03.009, 2008.

Biscoe, P. V., Cohen, Y., and Wallace, J. S.: Daily and Seasonal Changes of Water Potential in Cereals, Philosophical Transactions of the Royal Society of London. Series B, Biological Sciences, 273, 565-580, 1976.

Brooks, R. H., and Corey, A. T.: Hydraulic properties of porous media, Colorado State University, 1964.

Campbell, G. S., and Norman, J. M.: An Introduction To Environmental Biophysics, Secend Edition ed., Springer, New York, 2000.

Chen, F., Mitchell, K., Schaake, J., Xue, Y., Pan, H.-L., Koren, V., Duan, Q. Y., Ek, M., and Betts, A.: Modeling of land surface evaporation by four schemes and comparison with FIFE observations, Journal of Geophysical Research, 101(D3), 7251–7268, 10.1029/95JD02165, 1996.

Chen, F., and Dudhia, J.: Coupling an Advanced Land Surface–Hydrology Model with the Penn State–NCAR MM5 Modeling System. Part I: Model Implementation and Sensitivity, Monthly Weatherreview, 129, 569-585, 2001a.

Chen, F., and Dudhia, J.: Coupling an Advanced Land Surface–Hydrology Model with the Penn State–NCAR MM5 Modeling System. Part II: Preliminary Model Validation, Monthly Weatherreview, 129, 587-604, 2001b.

Daly, C., Gibson, W. P., Taylor, G. H., Johnson, G. L., and Pasteris, P.: A knowledgebased approach to the statistical mapping of climate, Climate Research, 22, 14, 2002.

Devonec, E., and Barros, A. P.: Exploring the transferability of a land-surface hydrology model, Journal of Hydrology, 265, 258-282, Doi: 10.1016/s0022-1694(02)00111-7, 2002.

Dickinson, R. E., Henderson-Sellers, A., Rosenzweig, C., and Sellers, P. J.: Evapotranspiration models with canopy resistance for use in climate models, a review, Agricultural and Forest Meteorology, 54, 373-388, Doi: 10.1016/0168-1923(91)90014-h, 1991.

Dickinson, R. E.: Land processes in climate models, Remote Sensing of Environment, 51, 27-38, Doi: 10.1016/0034-4257(94)00062-r, 1995.

Dingman, S. L.: Physical Hydrology, Prentice Hall, New Jersey, 2002.

Dirnböck, T., Dullinger, S., and Grabherr, G.: A regional impact assessment of climate and land-use change on alpine vegetation, Journal of Biogeography, 30, 401-417, 10.1046/j.1365-2699.2003.00839.x, 2003.

Essery, R. L. H., Best, M. J., Betts, R. A., and Cox, P. M.: Explicit Representation of Subgrid Heterogeneity in a GCM Land Surface Scheme, Journal of Hydrometeorology, 4, 530-543, 2003.

Famiglietti, J. S., and Wood, E. F.: Evapotranspiration and runoff from large land areas: Land surface hydrology for atmospheric general circulation models, Surveys in Geophysics, 12, 179-204, 10.1007/bf01903418, 1991.

Fried, J., Torn, M., and Mills, E.: The Impact of Climate Change on Wildfire Severity: A Regional Forecast for Northern California, Climatic Change, 64, 169-191, 10.1023/B:CLIM.0000024667.89579.ed, 2004.

Garcia-Quijano, J. F., and Barros, A. P.: Incorporating canopy physiology into a hydrological model: photosynthesis, dynamic respiration, and stomatal sensitivity, Ecological Modelling, 185, 29-49, DOI: 10.1016/j.ecolmodel.2004.08.024, 2005.

Ge, J., Qi, J., Lofgren, B. M., Moore, N., Torbick, N., and Olson, J. M.: Impacts of land use/cover classification accuracy on regional climate simulations, Journal of Geophysical Research, 112, 12, 10.1029/2006JD007404, 2007.

Gutman, G., and Ignatov, A.: Satellite-derived green vegetation fraction for the use in numerical weather prediction models, Advances in Space Research, 19, 477-480, 10.1016/s0273-1177(97)00058-6, 1997.

Haeberli, W., and Beniston, M.: Climate Change and Its Impacts on Glaciers and Permafrost in the Alps, Ambio, 27, 258-265, 1998.

Hagemann, S., Botzet, M., and Machenhauer, B.: The summer drying problem over south-eastern europe: sensitivity of the limited area model HIRHAM4 to improvements in physical parameterization and resolution, Physics and Chemistry of the Earth, Part B: Hydrology, Oceans and Atmosphere, 26, 391-396, Doi: 10.1016/s1464-1909(01)00024-7, 2001.

Hank, T. B.: A Biophysically Based Coupled Model Approach For the Assessment of Canopy Processes Under Climate Change Conditions, Fakultät für Geowissenschaften, Ludwig-Maximilians-Universität, München, 2008.

Henderson-Sellers, A., Dickinson, R. E., and Pitman, A. J.: Atmosphere-landsurface modelling, Mathematical and Computer Modelling, 21, 5-10, Doi: 10.1016/0895-7177(95)00045-4, 1995.

Henderson-Sellers, A., McGuffie, K., and Pitman, A. J.: The Project for Intercomparison of Land-surface Parametrization Schemes (PILPS): 1992 to 1995, Climate Dynamics, 12, 849-859, 1996.

Henderson-Sellers, A., Irannejad, P., and McGuffie, K.: Future desertification and climate change: The need for land-surface system evaluation improvement, Global and Planetary Change, 64, 129-138, DOI: 10.1016/j.gloplacha.2008.06.007, 2008.

IPCC: Climate Change 2007: Impacts, Adaptation and Vulnerability. Contribution of Working Group II to the Fourth Assessment Report of the Intergovernmental Panel on Climate Change. , Cambridge University Press, Cambridge, United Kingdom and New York, NY, USA., 976pp, 2007a.

IPCC: Climate Change 2007: The Physical Science Basis. Contribution of Working Group I to the Fourth Assessment Report of the Intergovernmental Panel on Climate Change. , Cambridge University Press, Cambridge, United Kingdom and New York, NY, USA., 996pp, 2007b.

Jacob, D., Bärring, L., Christensen, O. B., Christensen, J. H., Castro, M. d., Déqué, M., Giorgi, F., Hagemann, S., Hirschi, M., Jones, R., Kjellström, E., Lenderink, G., Rockel, B., Sánchez, E., Schär, C., Seneviratne, S. I., Somot, S., Ulden, A. v., and Hurk, B. v. d.: An inter-comparison of regional climate models for Europe: model performance in present-day climate, Climatic Change, 81, 31-52, 10.1007/s10584-006-9213-4, 2007.

Jacquemin, B., and Noilhan, J.: Sensitivity study and validation of a land surface parameterization using the HAPEX-MOBILHY data set, Boundary-Layer Meteorology, 52, 93-134, 10.1007/bf00123180, 1990.

Jarvis, P. G.: The Interpretation of the Variations in Leaf Water Potential and Stomatal Conductance Found in Canopies in the Field, Philosophical Transactions of the Royal Society of London. Series B, Biological Sciences, 273, 593-610, 1976.

Kalkstein, L., and Smoyer, K.: The impact of climate change on human health: Some international implications, Cellular and Molecular Life Sciences, 49, 969-979, 10.1007/bf02125644, 1993.

Koch, F., Prasch, M., Bach, H., Mauser, W., Appel, F., and Weber, M.: How Will Hydroelectric Power Generation Develop under Climate Change Scenarios? A Case Study in the Upper Danube Basin, MDPI Energies, 4, 33, 10.3390/en4101508, 2011.

Koster, R. D., and Suarez, M. J.: The components of a 'SVAT' scheme and their effects on a GCM's hydrological cycle, Advances in Water Resources, 17, 61-78, Doi: 10.1016/0309-1708(94)90024-8, 1994.

Koster, R. D., Dirmeyer, P. A., Guo, Z. C., Bonan, G., Chan, E., Cox, P., Gordon, C. T., Kanae, S., Kowalczyk, E., Lawrence, D., Liu, P., Lu, C. H., Malyshev, S., McAvaney, B., Mitchell, K., Mocko, D., Oki, T., Oleson, K., Pitman, A., Sud, Y. C., Taylor, C. M., Verseghy, D., Vasic, R., Xue, Y. K., Yamada, T., and Team, G.: Regions of strong coupling between soil moisture and precipitation, Science, 305, 1138-1140, 2004.

Kuchment, L. S., Demidov, V. N., and Startseva, Z. P.: Coupled modeling of the hydrological and carbon cycles in the soil-vegetation-atmosphere system, Journal of Hydrology, 323, 4-21, DOI: 10.1016/j.jhydrol.2005.08.011, 2006.

Kueppers, L. M., Snyder, M. A., Sloan, L. C., Cayan, D., Jin, J., Kanamaru, H., Kanamitsu, M., Miller, N. L., Tyree, M., Du, H., and Weare, B.: Seasonal temperature responses to land-use change in the western United States, Global and Planetary Change, 60, 250-264, DOI: 10.1016/j.gloplacha.2007.03.005, 2008.

Kunstmann, H., Jung, G., Wagner, S., and Clottey, H.: Integration of atmospheric sciences and hydrology for the development of decision support systems in sustainable water management, Physics and Chemistry of the Earth, Parts A/B/C, 33, 165-174, DOI: 10.1016/j.pce.2007.04.010, 2008.

Laprise, R.: Regional climate modelling, Journal of Computational Physics, 227, 3641-3666, DOI: 10.1016/j.jcp.2006.10.024, 2008.

Liston, G. E., and Elder, K.: A Meteorological Distribution System for High-Resolution Terrestrial Modeling (MicroMet), Journal of Hydrometeorology, 7, 17, 2006.

Loew, A.: Impact of surface heterogeneity on surface soil moisture retrievals from passive microwave data at the regional scale: The Upper Danube case, Remote Sensing of Environment, 112, 231-248, DOI: 10.1016/j.rse.2007.04.009, 2008.

Loew, A., Holmes, T., and Jeu, R. d.: The European heat wave 2003: early indicators from multisensoral microwave remote sensing?, Journal of Geophysical Research, 114, 10.1029/2008JD010533. , 2009.

Ludwig, R., and Mauser, W.: Modelling Catchment Hydrology within a GIS-based SVAT-model framework, , Hydrology and Earth System Sciences, 4, 239-249, 2000.

Ludwig, R., Probeck, M., and Mauser, W.: Mesoscale water balance modelling in the Upper Danube watershed using sub-scale land cover information derived from NOAA-AVHRR imagery and GIS-techniques, Physics and Chemistry of the Earth, Parts A/B/C, 28, 1351-1364, DOI: 10.1016/j.pce.2003.09.011, 2003a.

Ludwig, R., Taschner, S., and Mauser, W.: Modelling floods in the Ammer watershed – Experiences, Limitations and Challenges from a Coupled Meteo-Hydrological Model Approach, Hydrology and Earth System Sciences 7, 833-847, 2003b.

Ludwig, R., May, I., Turcotte, R., Vescovi, L., Braun, M., Cyr, J.-F., Fortin, L.-G., Chaumont, D., Biner, S., Chartier, I., Caya, D., and Mauser, W.: The role of hydrological model complexity and uncertainty in climate change impact assessment, Advances in Geosciences, 21, 63-71, 2009.

Mahrt, L., and Ek, M.: The Influence of Atmosperic Stability on Potential Evaporation, Journal of Climate and Applied Meteorology, 23, 222-234, 1984.

Marke, T.: Development and Application of a Model Interface To couple Land Surface Models with Regional Climate Models For Climate Change Risk Assessment In the Upper Danube Watershed, Fakultät für Geowissenschaften, Ludwig-Maximilians-Universität, München, 2008.

Marke, T., Mauser, W., Pfeiffer, A., and Zängl, G.: A pragmatic approach for the downscaling and bias correction of regional climate simulations – evaluation in hydrological modeling, Geosci. Model Dev. Discuss., 4, 45-63, 10.5194/gmdd-4-45-2011, 2011a.

Marke, T., Mauser, W., Pfeiffer, A., Zängl, G., and Jacob, D.: The effect of downscaling on river runoff modeling: a hydrological case study in the Upper Danube Watershed, Hydrol. Earth Syst. Sci. Discuss., 8, 6331–6384, 2011b.

Martin, P. H.: Land-surface characterization in climate models: biome-based parameter inference is not equivalent to local direct estimation, Journal of Hydrology, 212-213, 287-303, Doi: 10.1016/s0022-1694(98)00212-1, 1998.

Mauser, W., and Schädlich, S.: Modelling the spatial distribution of evapotranspiration on different scales using remote sensing data, Journal of Hydrology, 212-213, 250-267, Doi: 10.1016/s0022-1694(98)00228-5, 1998.

Mauser, W., and Bach, H.: PROMET - Large scale distributed hydrological modelling to study the impact of climate change on the water flows of mountain watersheds, Journal of Hydrology, 376, 362-377, DOI: 10.1016/j.jhydrol.2009.07.046, 2009.

Mc Gregor, J. L.: Regional Climate Modelling, Meterology and Atmospheric Physics, 63, 105-117, 1997.

Michalakes, J.: MM90: A scalable parallel implementation of the Penn State/NCAR Mesoscale Model (MM5), Parallel Computing, 23, 2173-2186, 1997.

Mitchell, K.: The Community Noah Land-Surface Model (LSM), 2005.

Molod, A., and Salmun, H.: A global assessment of the mosaic approach to modeling land surface heterogeneity, Journal of Geophysical Research, 107, 4217, 10.1029/2001jd000588, 2002.

Monteith, J. L.: Evaporation and the environment, Symposia of the Society for Experimental Biology, 19, 205-234, 1965.

Monteith, J. L., and Unsworth, M. H.: Principles of Environmental Physics, Third Edition ed., Elsevier, New York, 2008.

Muerth, M. J.: A Soil Temperature and Energy Balance Model for Integrated Assessment of Global Change Impacts at the regional scale, Fakultät für Geowissenschaften, Ludwig-Maximilians-Universität, München, 2008.

Myneni, R. B., Keeling, C. D., Tucker, C. J., Asrar, G., and Nemani, R. R.: Increased plant growth in the northern high latitudes from 1981 to 1991, Nature, 386, 698-702, 1997.

Noilhan, J., and Planton, S.: A Simple Parameterization of Land Surface Processes for Meteorological Models, Monthly Weather Review, 117, 14, 1989.

Orlowsky, B., and Seneviratne, S. I.: Statistical Analyses of Land–Atmosphere Feedbacks and Their Possible Pitfalls, Journal of Climate, 23, 3918-3932, 2010.

Parry, M., Rosenzweig, C., Iglesias, A., Fischer, G., and Livermore, M.: Climate change and world food security: a new assessment, Global Environmental Change, 9, Supplement 1, S51-S67, 10.1016/s0959-3780(99)00018-7, 1999.

Parry, M. L., Rosenzweig, C., Iglesias, A., Livermore, M., and Fischer, G.: Effects of climate change on global food production under SRES emissions and socio-economic scenarios, Global Environmental Change, 14, 53-67, 10.1016/j.gloenvcha.2003.10.008, 2004.

Patz, J. A., Campbell-Lendrum, D., Holloway, T., and Foley, J. A.: Impact of regional climate change on human health, Nature, 438, 310-317, 2005.

Pfeiffer, A., and Zängl, G.: Validation of climate-mode MM5-simulations for the European Alpine Region, Theoretical Applied Climatology, DOI 10.1007/s00704-009-0199-5, 2009.

Pitman, A. J.: The evolution of, and revolution in, land surface schemes designed for climate models, International Journal of Climatology, 23, 479-510, 10.1002/joc.893, 2003.

Polcher, J., McAvaney, B., Viterbo, P., Gaertner, M. A., Hahmann, A., Mahfouf, J. F., Noilhan, J., Phillips, T., Pitman, A., Schlosser, C. A., Schulz, J. P., Timbal, B., Verseghy, D., and Xue, Y.: A proposal for a general interface between land surface schemes and general circulation models, Global and Planetary Change, 19, 261-276, Doi: 10.1016/s0921-8181(98)00052-6, 1998.

Prasch, M., Strasser, U., and Mauser, W.: Validation of a physically based snow model for the simulation of the accumulation and ablation of snow (ESCIMO). in: Berchtesgaden National Park Research Report Proceedings of the Alpine Snow Workshop, Munich, 2006,

Prasch, M., Marke, T., Strasser, U., and Mauser, W.: Large scale integrated hydrological modelling of the impact of climate change on the water balance with DANUBIA, Advances in Science and Research, 7, 9, 10.5194/asr-7-61-2011, 2011.

Quintanar, A. I., Mahmood, R., Motley, M. V., Yan, J., Loughrin, J., and Lovanh, N.: Simulation of boundary layer trajectory dispersion sensitivity to soil moisture conditions: MM5 and Noah-based investigation, Atmospheric Environment, 43, 3774-3785, DOI: 10.1016/j.atmosenv.2009.04.005, 2009.

Richter, K., and Timmermans, W. J.: Physically based retrieval of crop characteristics for improved water use estimates, Hydrology and Earth System Sciences, 13, 663-674, 2009.

Schaake, J. C., Koren, V. I., Duan, Q.-Y., Mitchell, K., and Chen, F.: Simple water balance model for estimating runoff at different spatial and temporal scales, Journal of Geophysical Research, 101, 7461-7475, 10.1029/95jd02892, 1996.

Schär, C., Vidale, P. L., Lüthi, D., Frei, C., Häberli, C., Liniger, M. A., and Appenzeller, C.: The role of increasing temperature variability in European summer heatwaves, Nature, 427, 332-336, 2004.

Schulla, J., and Jasper, K.: Model description of WaSiM-ETH, Institute of Geography, ETH Zürich, 1999.
Seth, A., Giorgi, F., and Dickinson, R. E.: Simulating fluxes from heterogeneous land surfaces - explicit subgrid method employing the biosphere-atmosphere transfer scheme (BATS), Journal of Geophysical Research-Atmospheres, 99, 18651-18667, 1994.
Stocker, T.: Einführung in die Klimamodellierung, Universität Bern, Bern, 2004.
Strasser, U., and Mauser, W.: Modelling the Spatial and Temporal Variations of the Water Balance for the Weser Catchment 1965-1994, Journal of Hydrology, 254, 199-214, 2001.
Strasser, U., Franz, H., and Mauser, W.: Distributed modelling of snow processes in the Berchtesgaden National Park (Germany), in: Berchtesgaden National Park Research Report Proceedings of the Alpine Snow Workshop, Munich, 2007, 117–130,
Timbal, B., and Henderson-Sellers, A.: Intercomparisons of land-surface parameterizations coupled to a limited area forecast model, Global and Planetary Change, 19, 247-260, Doi: 10.1016/s0921-8181(98)00051-4, 1998.
Uppala, S. M., Kallberg, P. W., Simmons, A. J., Andrae, U., Bechtold, V. D. C., Fiorino, M., Gibson, J. K., Haseler, J., Hernandez, A., Kelly, G. A., Li, X., Onogi, K., Saarinen, S., Sokka, N., Allan, R. P., Andersson, E., Arpe, K., Balmaseda, M. A., Beljaars, A. C. M., Berg, L. V. D., Bidlot, J., Bormann, N., Caires, S., Chevallier, F., Dethof, A., Dragosavac, M., Fisher, M., Fuentes, M., Hagemann, S., Hólm, E., Hoskins, B. J., Isaksen, L., Janssen, P. A. E. M., Jenne, R., McNally, A. P., Mahfouf, J.-F., Morcrette, J.-J., Rayner, N. A., Saunders, R. W., Simon, P., Sterl, A., Trenberth, K. E., Untch, A., Vasiljevic, D., Viterbo, P., and Woollen, J.: The ERA-40 Re-analysis., Quarterly Journal of the Royal Meteorological Society,, 131, 2961-3012, 10.1256/qj.04.176, 2005.
Wagener, T., Franks, S., Gupta, H. V., Bogh, E., Bastidas, L., Nobre, C., and Galvao, C. D. O.: Regional Hydrological Impacts of Climatic Change - Impact Assessment and Decision Making, IAHS Publication, edited by: Thorsten Wagener, Stewart Franks, Hoshin V. Gupta, Eva Bogh, Luis Bastidas, Carlos Nobre, and Galvao, C. D. O., International Association of Hydrological Sciences (IAHS), Wallingford, 359 pp., 2005.
Wagner, S., Kunstmann, H., Bárdossy, A., Conrad, C., and Colditz, R. R.: Water balance estimation of a poorly gauged catchment in West Africa using dynamically downscaled meteorological fields and remote sensing information, Physics and Chemistry of the Earth, Parts A/B/C, 34, 225-235, DOI: 10.1016/j.pce.2008.04.002, 2009.
Weber, M., Braun, L., Mauser, W., and M., P.: Contribution of rain, snow- and icemelt in the Upper Danube discharge today and in the future, Geografia Fisica e Dinamica Quaternaria, 33, 221-230, 2010.
Wood, E. F., Lettenmaier, D. P., Liang, X., Lohmann, D., Boone, A., Chang, S., Chen, F., Dai, Y., Dickinson, R. E., Duan, Q., Ek, M., Gusev, Y. M., Habets, F., Irannejad, P., Koster, R., Mitchel, K. E., Nasonova, O. N., Noilhan, J., Schaake, J., Schlosser, A., Shao, Y., Shmakin, A. B., Verseghy, D., Warrach, K., Wetzel, P., Xue, Y., Yang, Z.-L., and Zeng, Q.-c.: The Project for Intercomparison of Land-surface Parameterization Schemes (PILPS) Phase 2(c) Red-Arkansas River basin experiment:: 1. Experiment description and summary intercomparisons, Global and Planetary Change, 19, 115-135, Doi: 10.1016/s0921-8181(98)00044-7, 1998.
Yang, Z.-L., Dickinson, R. E., Shuttleworth, W. J., and Shaikh, M.: Treatment of soil, vegetation and snow in land surface models: a test of the Biosphere-Atmosphere Transfer Scheme with the HAPEX-MOBILHY, ABRACOS and Russian data, Journal of Hydrology, 212-213, 109-127, Doi: 10.1016/s0022-1694(98)00205-4, 1998.
Yu, Z.: Assessing the response of subgrid hydrologic processes to atmospheric forcing with a hydrologic model system, Global and Planetary Change, 25, 1-17, Doi: 10.1016/s0921-8181(00)00018-7, 2000.

Zabel, F., Hank, T. B., and Mauser, W.: Improving arable land heterogeneity information in available land cover products for land surface modelling using MERIS NDVI data, Hydrology and Earth System Sciences, 14, 2073-2084, doi:10.5194/hess-14-2073-2010, 2010.

Zampieri, M., Giorgi, F., Lionello, P., and Nikulin, G.: Regional climate change in the Northern Adriatic, Physics and Chemistry of the Earth, Parts A/B/C, In Press, Corrected Proof, DOI: 10.1016/j.pce.2010.02.003, 2011.

Zängl, G.: An improved method for computing horizontal diffusion in a sigma-coordinate model and its application to simulations over mountainous topography., Monthly Weather Review, 130, 1423-1432, 2002.

Zeng, X. M., Zhao, M., Su, B. K., Tang, J. P., Zheng, Y. Q., Zhang, Y. J., and Chen, J.: Effects of the land-surface heterogeneities in temperature and moisture from the "combined approach" on regional climate: a sensitivity study, Global and Planetary Change, 37, 247-263, Doi: 10.1016/s0921-8181(02)00209-6, 2003.